UiT
THE ARCTIC
UNIVERSITY
OF NORWAY

Faculty of Science and Technology
Department of Physics and Technology

Advancing Segmentation and Unsupervised Learning Within the Field of Deep Learning

—

Michael Kampffmeyer, UiT Machine Learning Group

A dissertation for the degree of Philosophiae Doctor — August 2018

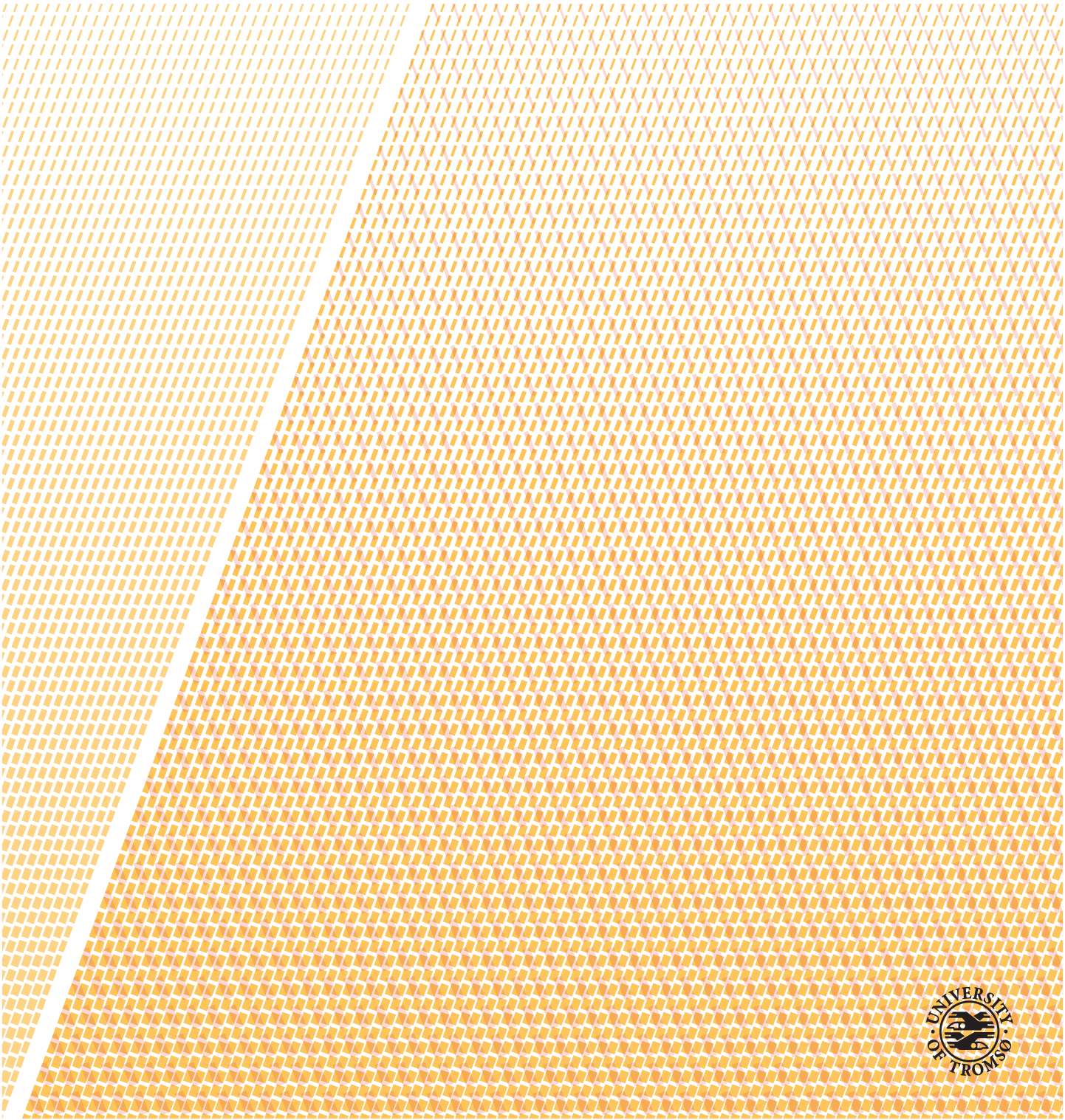

Abstract

Due to the large improvements that deep learning based models have brought to a variety of tasks, they have in recent years received large amounts of attention. However, these improvements are to a large extent achieved in supervised settings, where labels are available, and initially focused on traditional computer vision tasks such as visual object recognition. Specific application domains that consider images of large size and multi-modal images, as well as applications where labeled training data is challenging to obtain, has instead received less attention.

This thesis aims to fill these gaps from two overall perspectives. First, we advance segmentation approaches specifically targeted towards the applications of remote sensing and medical imaging. Second, inspired by the lack of labeled data in many high-impact domains, such as medical imaging, we advance four unsupervised deep learning tasks: domain adaptation, clustering, representation learning, and zero-shot learning.

The works on segmentation address the challenges of class-imbalance, missing data-modalities and the modeling of uncertainty in remote sensing. Founded on the idea of pixel-connectivity, we further propose a novel approach to saliency segmentation, a common pre-processing task. We illustrate that phrasing the problem as a connectivity prediction problem, allows us to achieve good performance while keeping the model simple. Finally, connecting our work on segmentation and unsupervised deep learning, we propose an approach to unsupervised domain adaptation in a segmentation setting in the medical domain.

Besides unsupervised domain adaptation, we further propose a novel approach to clustering based on integrating ideas from kernel methods and information theoretic learning achieving promising results. Based on our intuition that meaningful representations should incorporate similarities between data points, we further propose a kernelized autoencoder. Finally, we address the task of zero-shot learning based on improving knowledge propagation in graph convolutional neural networks, achieving state-of-the-art performance on the 21K class ImageNet dataset.

Acknowledgements

First and foremost I would like to thank Professor Robert Jenssen for being the best supervisor I could have asked for. Robert's guidance and support are what made this thesis possible and I am grateful for all the time and effort that he spent on teaching me the ways of academia. A special thanks also to my co-supervisor Dr. Arnt-Børre Salberg for all the insightful discussions and all his advice.

I am grateful to Professor Eric P. Xing for giving me the opportunity to spend 10 months in his lab at Carnegie Mellon University. It was a truly inspiring and memorable experience. I would like to thank Dr. Xiaodan Liang for mentoring me while I was there and would like to thank everyone in the SAILING Lab, and all the other visitors in the visitors office, for making it so enjoyable. Special thanks to Yujia for her wonderful sense of humor and the countless meals, which provided a nice break from work.

I would also like to express my gratitude to everyone in the Machine Learning Group at UiT. It has been fun to see it grow from Jonas, Karl Øyvind, Sigurd, and Filippo to so many people that I do not have space to mention them all. Further, I am particularly grateful to all my co-authors and colleagues. It has been amazing working with so many brilliant people and I look forward to continuing our collaborations. I would also like to thank Filippo, Karl Øyvind, and Einar for allowing me to distribute all my belongings in their houses while I was at CMU.

I want to thank my committee members Associate Professor Devis Tuia, Dr. Wojciech Samek, and Professor Fred Godtliebsen for making time to read the thesis and attend the defense.

Special shoutout to Hansi & Family for all their dinner invitations. Building trains with Ciljan and Otelie is a nice change of pace from busy days at the office. Last but definitely not least, I would like to thank my family for their continued support!

Michael Kampffmeyer
Tromsø, August 2018

Contents

List of Figures

List of Abbreviations

ADDA adversarial discriminative domain adaptation

AE Autoencoder

BM Boltzmann Machine

CAE Contractive Autoencoder

CNN Convolutional Neural Network

CS Cauchy-Schwartz

dAE Denoising Autoencoder

FCN Fully Convolutional Network

GAN Generative adversarial network

GCN Graph Convolutional Neural Network

GPU Graphics Processing Unit

KL Kullback-Leibler

MLP Multilayer Perceptron

MSE Mean Square Error

PCA Principal Component Analysis

RBM Restricted Boltzmann Machine

ReLU Rectified Linear Unit

sAE Sparse Autoencoder

SdAE Stacked Denoising Autoencoder

SGD Stochastic Gradient Descent

SVM Support Vector Machine

VAE Variational Autoencoder

1 Introduction

In the past few years, impressive results have been achieved on various tasks using deep learning, such as for example speech recognition [Bahdanau et al., 2016, Hinton et al., 2012], image classification [He et al., 2016, Krizhevsky et al., 2012], object detection [Girshick, 2015, Ren et al., 2017], image segmentation [Chen et al., 2018, He et al., 2017, Long et al., 2015a], video analysis [Karpathy et al., 2014, Zhang et al., 2018a,b], and time-series analysis [Bianchi et al., 2017, Chang et al., 2017]. Especially in the computer vision domain, convolutional neural networks have revolutionized the field and deep learning is nowadays used by many people on a daily basis [LeCun et al., 2015]. They often outperform more traditional approaches as they do not rely on hand-crafted features but are able to learn meaningful task-dependent feature representations from data at the same time as they learn how to perform the task (for instance classification).

The aim of this thesis is to contribute to the advances of deep learning by addressing some key challenges in the field. These challenges are briefly outlined in the next section and will be treated in more detail in the corresponding papers. An overview of the different aspects that have been addressed is displayed in Figure 1.1 to guide the reader.

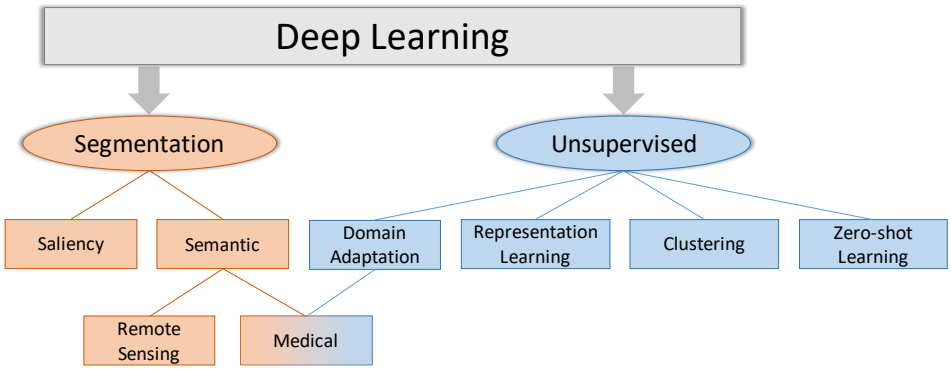

Figure 1.1: An overview of the topics addressed in this thesis.

1.1 Key Challenges

Many of these aforementioned advances have been focusing on images taken with hand-held cameras, however, these images and the requirements for processing these can differ considerably from other imaging domains. For instance, objects of interest are generally of considerable size and commonly only consist of bands in the visible spectrum.

Semantic segmentation is an important field in remote sensing and is used for tasks such as environmental monitoring, forestry, disaster monitoring, agriculture and urban planning [Maggiori et al., 2017, Salberg et al., 2017]. However, relatively little work has been done on developing deep learning methods that are tailored to the distinct properties that these images have and which differ from the more traditionally used images. These properties include the larger image size, the potentially small objects of interest and, possibly, a diverse set of data modalities [Zhu et al., 2017]. The difference is illustrated in Figure 1.2, which shows a typical image that can be encountered in remote sensing and an image that represents the type of image that has received most focus in computer vision in the recent years. Not accounting for these differences in image properties has, for instance, led to poor performance on classes that contain only a small number of pixels [Marmanis et al., 2018]. Effectively addressing these differences in order to design more accurate and fitting approaches is a promising direction.

Compared to semantic segmentation, salient segmentation aims to segment out attention-grabbing regions and is a critical task as it builds the foundation of many high-level computer vision applications. For instance, segmentation in remote sensing and the medical domain has been performed with the help of salient segmentation [Chen and Lee, 2012, Sharma and Ghosh, 2015]. Other applications include object detection [Navalpakkam and Itti, 2006], video sum-

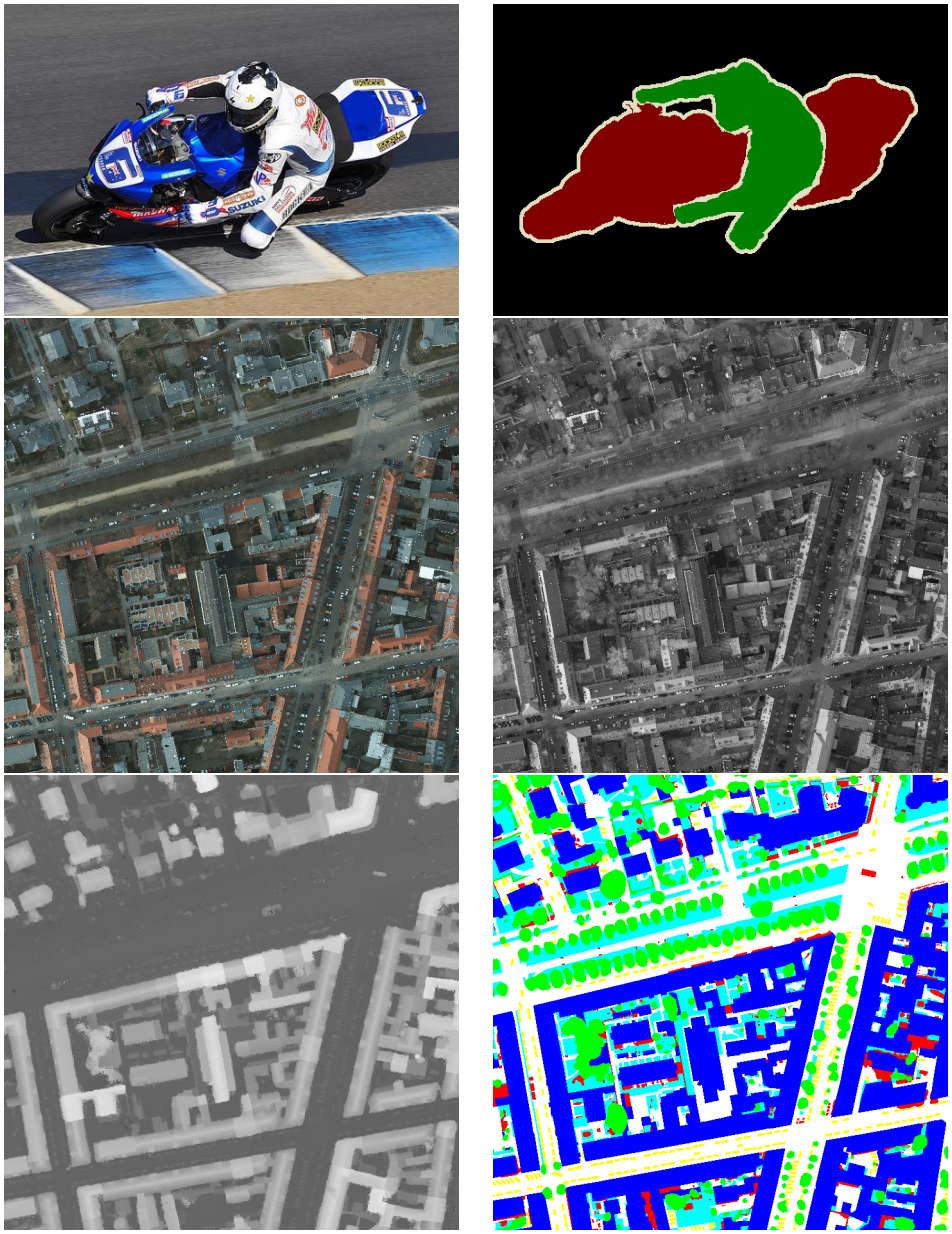

Figure 1.2: The first row displays an image and the segmentation ground truth from the Pascal VOC dataset [Everingham et al., 2015] and represents the typical images considered in computer vision. The second and third row show a more typical remote sensing image. From left to right, top to bottom: RGB image, Infrared (IR) image, Digital Surface Model (DSM) and ground truth. The image has been taken from the ISPRS benchmark dataset provided by the German Association of Photogrammetry and Remote Sensing [Cramer, 2010] and illustrates the difference in image size (500×342 compared to 6000×6000 pixels), the importance of small objects, and the availability of multiple modalities in remote sensing.

marization [Ma et al., 2002] and face detection [Liu et al., 2017]. In recent years, salient segmentation has been approached using the same methods as semantic segmentation and the architectures have ever grown in complexity, achieving incremental improvements at the cost of considerable model complexity. Since salient segmentation is used in such a large range of applications, approaches specifically designed for the task of salient segmentation that achieve good performance at lower computational cost are desirable.

Further, most of the advances in deep learning have been achieved by supervised approaches, utilizing large amounts of labeled training data. Unsupervised deep learning, the process of learning from unlabeled data, instead, is still in its infancy. In settings where labeled data is limited, supervised models are likely to overfit to the available dataset and will not generalize well to additional data. However, there is a large untapped potential due to the availability of large amounts of unlabeled data and unsupervised learning is expected to become more and more important in the near future [LeCun et al., 2015]. One such domain of limited training data is the medical domain. Medical imaging is an important domain that has recently been shown to benefit from deep learning [Dong et al., 2018, Esteva et al., 2017, Litjens et al., 2017], however, data is generally limited due to the tremendous cost of collecting and labeling it. Additionally, data taken from different hospitals often differ with respect to noise levels, contrast and resolution, making it challenging to exploit openly available data.

1.2 Key Objectives

In this thesis, we focus on the above-mentioned challenges in deep learning by first addressing domain specific problems related to segmentation in two important imaging domains, namely, remote sensing and medical imaging. We then propose new approaches to unsupervised deep learning. The key objectives of the thesis can be summarized as

- Target key-challenges for segmentation in the remote sensing and medical domain.
- Rethink the approach to salient segmentation.
- Design approaches to learn from unlabeled data in the deep learning framework.

1.3 Key Solutions

In remote sensing, we investigate the use of Convolutional Neural Networks (CNNs) for the task of urban area segmentation and explore how to reduce the problem of class imbalance, by accounting for class imbalance in the loss function. We further investigate how uncertainty can be assessed (Paper I). The diverse set of data modalities in remote sensing introduces another problem as not all data modalities might be available during the model's inference phase. We examine how this issue can be addressed in Paper II.

In the medical domain, when performing chest organ semantic segmentation, we propose an unsupervised domain adaptation approach in Paper III to address the problem of limited available labeled data. This work further connects to the third key objective to develop unsupervised deep learning approaches and links the two overall objectives in the thesis to advance segmentation and unsupervised learning within deep learning.

In an effort to find a more fitting approach to salient segmentation, we propose a novel approach based on modeling relationships between neighboring pixels and phrasing the salient segmentation task as a pixel-connectivity prediction task (Paper IV).

In order to address the issue of missing labels, we propose new approaches for unsupervised deep learning by integrating among others, ideas from more traditional machine learning, such as kernel methods and information theoretic learning. These traditional methods have had large success for unsupervised learning tasks and we hypothesize that unsupervised deep learning techniques can benefit from some aspects of these methods. Here we specifically focus on four different sub-areas of unsupervised learning. Besides the aforementioned unsupervised domain adaptation (Paper III), we design a method for clustering, that aims to find structures in unlabeled data (Paper VI). In Paper V, we propose an approach to unsupervised representation learning that learns efficient latent representations of data. Finally, in Paper VII, we address the task of zero-shot image classification, the task where classification models are extended to allow the classification of images to previously unseen classes based on the semantic relationships between seen and unseen classes.

1.4 Brief summary of papers

This section provides a list of papers included in this thesis, each with a brief summary. A list over other articles published over the course of this three-year PhD project is presented in the next section. Figure 1.3a provides an overview

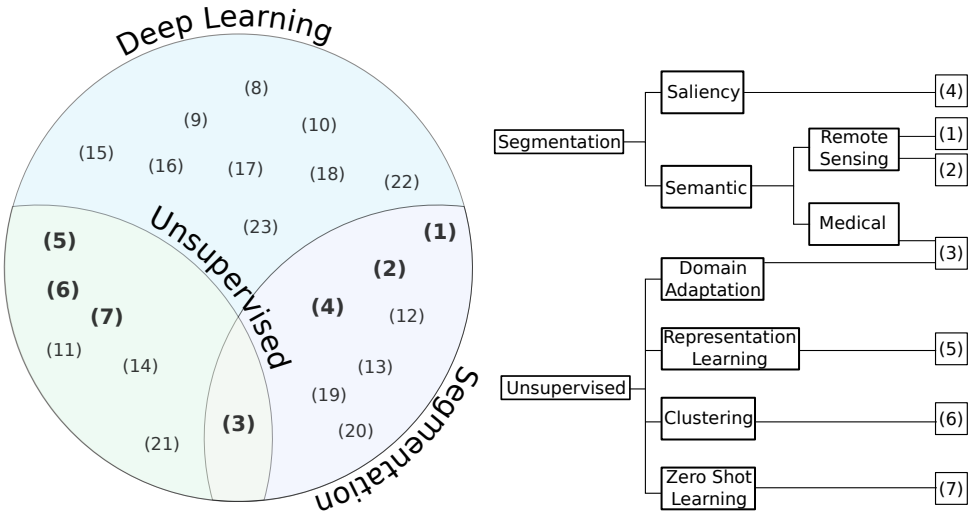

(a) Overview of papers **(b)** Included paper hierarchy

Figure 1.3: For the overview figure, the two overlapping inner circles illustrate which publications consider aspects in segmentation and which are based on unsupervised learning. The seven papers included in the thesis are highlighted in bold. The numbers correspond to the number in the publication list. The paper hierarchy illustrates the sub-fields of unsupervised learning and segmentation that are being considered in the included papers.

of the publications. Figure 1.3b provides a more detailed overview over the included papers and illustrates the sub-topics of segmentation and unsupervised learning that are being considered.

1. Michael Kampffmeyer, Arnt-Børre Salberg, and Robert Jenssen. "**Semantic segmentation of small objects and modeling of uncertainty in urban remote sensing images using deep convolutional neural networks.**" Proceedings of the IEEE Conference on Computer Vision and Pattern Recognition Workshops, 2016.

2. Michael Kampffmeyer, Arnt-Børre Salberg, and Robert Jenssen. "**Urban Land Cover Classification with Missing Data Modalities Using Deep Convolutional Neural Networks.**", IEEE Journal of Selected Topics in Applied Earth Observations and Remote Sensing, 2018.

3. Nanqing Dong, Michael Kampffmeyer, Xiaodan Liang, Zeya Wang, Wei Dai, and Eric P. Xing. "**Unsupervised Domain Adaptation for Automatic Estimation of Cardiothoracic Ratio.**", Proceedings of the International Conference on Medical Image Computing and Computer Assisted Intervention, 2018.

4. Michael Kampffmeyer, Nanqing Dong, Xiaodan Liang, Yujia Zhang, and Eric P. Xing. "**ConnNet: A Long-Range Relation-Aware Pixel-Connectivity Network for Salient Segmentation.**" arXiv preprint arXiv:1804.07836, 2018 (submitted to IEEE Transactions on Image Processing).

5. Michael Kampffmeyer, Sigurd Løkse, Filippo M Bianchi, Robert Jenssen, and Lorenzo Livi. "**The Deep Kernelized Autoencoder.**", Applied Soft Computing, 2018.

6. Michael Kampffmeyer, Sigurd Løkse, Filippo M Bianchi, Lorenzo Livi, Arnt-Børre Salberg, and Robert Jenssen. "**Deep Divergence-Based Approach to Clustering.**", submitted to Neural Networks.

7. Michael Kampffmeyer, Yinbo Chen, Xiaodan Liang, Hao Wang, Yujia Zhang, and Eric P. Xing. "**Rethinking Knowledge Graph Propagation for Zero-Shot Learning.**" arXiv preprint arXiv:1805.11724, 2018 (submitted to Neural Information Processing Systems 2018).

Paper I and II: Consider semantic segmentation in remote sensing. Paper I compares so-called patch-based approaches with fully convolutional approaches, proposes the use of a class balanced cost function to address the class imbalance problem, and investigates the use of uncertainty modeling for urban land cover classification in remote sensing. Paper II instead addresses the problem of missing data modalities. As many approaches make use of data-fusion to improve overall accuracy, this raises the question of what can be done when certain data modalities are missing during testing. We illustrate a possible solution for situations where multiple or a single modality are completely missing or only missing for a few images during testing.

Paper III: Proposes a method to perform unsupervised domain adaptation for estimation of the cardiothoracic ratio, a key indicator for cardiomegaly (heart enlargement), which is associated with a high risk of sudden cardiac death. We address the fact that labeled training data is difficult and expensive to obtain, and the fact that data from different hospitals exhibit differences in noise levels, contrast, and resolution. Based on adversarial learning, an unsupervised approach is proposed that can be trained with data from one hospital and still provides good performance on data from another hospital. We further illustrate that the method can also be used for semi-supervised learning.

Paper IV: Presents a new approach to salient segmentation, segmentation of the attention-grabbing objects in an image. Unlike recent state-of-the-art approaches, who approach this task as a binary segmentation task (foreground vs. background segmentation) and make network architectures more and more

complicated, the problem is rephrased as a connectivity prediction problem. This allows for better performance with a simpler model.

Paper V: Develops a deep kernelized auto-encoder architecture that incorporates a kernel-alignment based regularization term. Efficient data representations can be learned by exploiting the similarity between data in the input space and we illustrate that the deep kernelized autoencoder achieves promising results. It further, introduces a link between kernel methods and deep learning.

Paper VI: Incorporates more traditional machine learning techniques such as kernel methods and information theoretic learning into deep learning. It proposes an unsupervised deep architecture that achieved state-of-the-art clustering results on challenging problems. The commonly used supervised loss function is replaced by an information theoretic divergence unsupervised loss function that finds the underlying structures (clusters) in data by enforcing separation between clusters and compactness within clusters.

Paper VII: This paper focuses on zero-shot learning. Based on recent developments in the field of Graph Convolutional Neural Networks (GCNs), we propose an Attentive Dense Graph Propagation Module that allows us to achieve state-of-the-art performance on large-scale zero-shot datasets by exploiting knowledge graph information.

1.5 Other papers

8. Jonas N Myhre, Michael Kampffmeyer, and Robert Jenssen. "**Ambient space manifold learning using density ridges.**", Geometry in Machine Learning Workshop, International Conference on Machine Learning, 2016.

9. Filippo Maria Bianchi, Michael Kampffmeyer, Enrico Maiorino, and Robert Jenssen. "**Temporal Overdrive Recurrent Neural Network.**", 2017 International Joint Conference on Neural Networks, 2017.

10. Jonas N. Myhre, Michael Kampffmeyer, and Robert Jenssen. "**Density ridge manifold traversal.**", 2017 IEEE International Conference on Acoustics, Speech and Signal Processing, 2017.

11. Michael Kampffmeyer, Sigurd Løkse, Filippo M Bianchi, Robert Jenssen, and Lorenzo Livi. "**Deep Kernelized Autoencoders.**" Scandinavian Conference on Image Analysis. Springer, 2017.

12. Arnt-Børre Salberg, Øivind Due Trier, and Michael Kampffmeyer. "**Large-Scale Mapping of Small Roads in Lidar Images Using Deep Convolutional Neural Networks.**" Scandinavian Conference on Image Analysis. Springer, 2017.

13. Michael Kampffmeyer, Arnt-Børre Salberg, and Robert Jenssen. "**Urban Land Cover Classification with Missing Data Using Deep Convolutional Neural Networks.**", IEEE International Geoscience and Remote Sensing Symposium, 2017.

14. Michael Kampffmeyer, Sigurd Løkse, Filippo M Bianchi, Lorenzo Livi, Arnt-Børre Salberg, and Robert Jenssen. "**Deep Divergence-based Clustering.**", IEEE International Workshop on Machine Learning for Signal Processing, 2017.

15. Filippo Maria Bianchi, Enrico Maiorino, Michael Kampffmeyer, Antonello Rizzi, and Robert Jenssen. "**Recurrent Neural Networks for Short-Term Load Forecasting An Overview and Comparative Analysis.**", SpringerBriefs in Computer Science, 2017.

16. Andreas S Strauman, Filippo M Bianchi, Karl Øyvind Mikalsen, Michael Kampffmeyer, Cristina Soguero-Ruiz, and Robert Jenssen. "**Classification of postoperative surgical site infections from blood measurements with missing data using recurrent neural networks.**", IEEE International Conference on Biomedical and Health Informatics, 2018.

17. Mads A Hansen, Karl Øyvind Mikalsen, Michael Kampffmeyer, Cristina Soguero-Ruiz, and Robert Jenssen. "**Towards Deep Anchor Learning.**", IEEE International Conference on Biomedical and Health Informatics, 2018.

18. Yujia Zhang, Michael Kampffmeyer, Xiaodan Liang, Min Tan, and Eric P. Xing. "**Query-Conditioned Three-Player Adversarial Network for Video Summarization.**", British Machine Vision Conference, 2018.

19. Kristoffer Knutsen Wickstrøm, Michael Kampffmeyer, and Robert Jenssen. "**Uncertainty Modeling And Interpretability In Convolutional Neural Networks For Polyp Segmentation.**", IEEE International Workshop on Machine Learning for Signal Processing, 2018.

20. Nanqing Dong, Michael Kampffmeyer, Xiaodan Liang, Zeya Wang, Wei Dai, and Eric P. Xing. "**Reinforced Auto-Zoom Net: Towards Accurate and Fast Breast Cancer Segmentation in Whole-slide Images.**", Proceedings of the 4th Workshop on Deep Learning in Medical Image Anal-

ysis, 2018.

21. Filippo Maria Bianchi, Lorenzo Livi, Karl Øyvind Mikalsen, Michael Kampffmeyer, and Robert Jenssen. "**Learning representations for multivariate time series with missing data using Temporal Kernelized Autoencoders.**", arXiv preprint arXiv:1805.03473, 2018 (submitted to Neural Networks).

22. Yujia Zhang, Michael Kampffmeyer, Xiaodan Liang, Dingwen Zhang, Min Tan, and Eric P. Xing. "**DTR-GAN: Dilated Temporal Relational Adversarial Network for Video Summarization.**", arXiv preprint arXiv:1804.11228, 2018 (submitted to IEEE Transactions on Image Processing).

23. Rogelio Andrade Mancisidor, Michael Kampffmeyer, Kjersti Aas, and Robert Jenssen. "**Segment-Based Credit Scoring Using Latent Clusters in the Variational Autoencoder.**", arXiv preprint arXiv:1806.02538, 2018 (submitted to Information Sciences).

1.6 Reading guide

The thesis is organized into three parts, *methodology*, *summary of research*, and *included papers*.

The *methodology* part provides the theoretical background for the research presented in this thesis. Chapter 2 provides a short overview of deep learning and introduces Convolutional Neural Networks, Graph Convolutional Networks, Autoencoders, and Generative Adversarial Networks and is relevant background material for all papers. Chapter 3 introduces the tasks of semantic segmentation and salient segmentation and presents how these tasks are addressed using deep learning. This is relevant for Papers I-IV. Chapter 4 introduces unsupervised learning, briefly summarizing the tasks of clustering, domain adaptation, representation learning, and zero-shot learning and is relevant for Paper III and Papers V-VII. Finally, Chapter 5 provides background on kernel methods and information theoretic learning, which is relevant for Papers V and VI.

The *summary of research* part provides a short overview of the scientific contribution of each paper in this thesis as well as concluding remarks and a discussion of future directions. Research papers are included in the *included papers* part.

Part I

Methodology and context

2

Deep Learning

Deep learning techniques can today be encountered in many everyday applications ranging from speech and handwritten character recognition to various image and object detection tasks. They are representation-learning techniques, accepting raw data as input and being trained to discover useful features, instead of relying on hand-tuned feature extractors. Deep learning architectures consist of multiple layers, each consisting of simple modules that are subject to learning, and learn representations, each layer yielding a slightly more abstract and "useful" representation.

The idea of learning representations has been around since the late 1950's, when the perceptron algorithm was proposed by Frank Rosenblatt and led to the rise of many perceptron based methods, however, it initially only delivered minor successes [Rosenblatt, 1958]. In 1969 Minsky and Papert demonstrated that a perceptron is not able to solve simple non-linear problems such as the XOR problem, and argued the fact that computational resources, as well as effective training procedures for large multi-layer networks, did not exist [Minsky and Seymour, 1969]. This led to a drought in the field of neural networks until an effective algorithm, the backpropagation algorithm, for training these networks using stochastic gradient descent was independently discovered by multiple research groups between 1974 and 1986 [LeCun et al., 2015]. Backpropagation computes the gradient of the objective function with respect to all weights and uses this gradient to update the weights in all layers using one of several proposed gradient descent approaches.

After minor successes of shallow neural networks with backpropagation on, among others, handwritten digit recognition tasks using a technique called Convolutional Neural Networks (CNNs), most researchers forsake neural networks for more successful methods, such as the Support Vector Machines (SVMs) [Boser et al., 1992] and Random Forests [Ho, 1995]. Neural networks appeared to commonly get trapped in local minima, thus yielding weight configurations that on a local scale of the loss surface achieve a minimum, but on the global scale are far from optimal. Recent results by Dauphin et al. [2014] and Choromanska et al. [2014] suggest that this might have been a misconception and that the loss surface in deep neural networks generally consists mainly of bad saddle-points, as most local minima in large networks lie close to the global minima. Another problem of neural networks was the vanishing and exploding gradient problem, where the gradient either diminishes or explodes as it propagates through the network as part of backpropagation.

First in 2006, the interest in deep neural network architectures was restored by the development of unsupervised learning techniques that could be used to effectively pretrain deep networks. These techniques can be divided into two main classes, probabilistic models, the most prominent of these methods being the Restricted Boltzmann Machines (RBMs) [Hinton, 2002, Smolensky, 1986] and the Variational Autoencoders (VAEs) [Kingma and Welling, 2014], and methods that directly learn a parametric mapping from the input to the representation, such as autoencoders [Ballard, 1987, Vincent et al., 2010]. Together with the pretraining idea, advances of fast and programmable Graphics Processing Units (GPUs), larger available datasets, as well as some general techniques to the neural network concept that addressed gradient propagation issues, they led to deep neural networks beating state-of-the-art results on speech recognition tasks [Dahl et al., 2012, Mohamed et al., 2012]. Already in 2012 speech recognition systems based on neural networks were deployed to consumers (e.g. android mobile phones) [LeCun et al., 2015].

In 2012 another breakthrough happened when a CNN with $\approx$ 60 million weights won the ImageNet competition, in which a training set of $\approx$1.2 million images containing 1000 classes had to be used to train an image classifier [Krizhevsky et al., 2012]. Since then CNNs have been widely adopted and are now the dominant approach for most image and object recognition tasks.

In this chapter, we briefly review the deep learning approaches that provide the backbone of this thesis.

2.1 Fully Connected Neural Networks

Fully Connected Neural Networks or Multilayer Perceptrons (MLPs), represent the general foundation of the deep learning architectures and methods presented in this thesis. They consist of a composition of many simple mappings and transformations, which are hierarchically organized in several layers. This allows the modeling of arbitrary complex deterministic functions.

In this section, we will limit our discussion of MLPs to the task of supervised classification. In supervised learning the learning problem can be defined as follows: given an input space X, an output space Y and a data distribution D over $X \times Y$ that contains the data that is being observed, the learning procedure attempts to find a function $f : X \to Y$ that minimizes a loss function $L(f(\boldsymbol{x}), y)$. In classification, the loss function quantifies how well the network is able to map $\boldsymbol{x}$ to class y. In machine learning the optimization problem generally involves a finite dataset of $D = \{(\boldsymbol{x}_i, y_i)\ i = 1, ..., N\}$ that is used to train the model. Here, $(\boldsymbol{x}_i, y_i)$ corresponds to the ith training sample of data distribution D. The objective is to learn a function that minimizes the loss, but at the same time and more importantly generalizes well to a new set of previously unseen data points drawn from D.

The MLP consists of multiple layers of units (also called neurons), which are organized in a hierarchy as illustrated in Figure 2.1. MLPs consist of one input and one output layer, where the input layer represents the feature vectors of the data that is to be classified and the result of the last layer corresponds to the expected classification for the feature vector. Additionally, they consist of one or more hidden layers, where the correct values for the features are unknown and need to be found during training. Each of these hidden layers transforms or maps the data from the previous representation to a new representation, which, when optimizing for a classification task, will make the data points easier to classify. These representations become potentially more and more abstract as the network depth increases, allowing the last layer to separate the final representation as best as possible using a hyperplane.

Each unit in the hidden and output layer consists of a weighted sum of the units input values (including bias). Additionally, a nonlinearity is used approximating the unit step function to indicate unit activation. The most common nonlinearity has historically been the sigmoid function $\sigma = g_{sigmoid}(x) = \frac{1}{1+e^{-x}}$, such that the output of a unit i in layer l is defined by

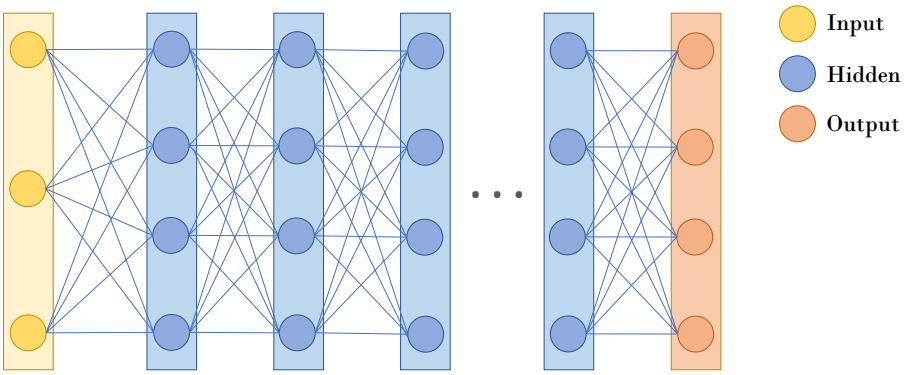

Figure 2.1: The figure displays an example architecture of a MLP with three input units and four output neurons.

$$y_i^l = \sigma(b_i^l + \sum_{j=1}^{N} w_{ij}^l y_j^{l-1}) \,, \tag{2.1}$$

where b_i is the bias term, w_{ij} is the weight between layer input y_j^{l-1} and layer output y_i^l. However, in recent years the nonlinearity has been to a large extent replaced by Rectified Linear Units (ReLUs) [Glorot et al., 2011], which have more preferable properties when training MLPs with a larger number of hidden layers. The ReLU is defined as $g_{ReLU}(x) = \max(0, x)$ leading to sparse activation patterns and better gradient flow [Glorot et al., 2011]. In the classification setting, the final layer, commonly makes use of a softmax layer. The softmax function, $g_{Softmax}(\boldsymbol{x})_j = \frac{e^{x_j}}{\sum_{k=1}^{K} e^{x_k}}$, squashes the values of the output neurons into the range (0,1) and ensures that they sum up to 1.

A common loss function L that is often used in classification settings is the cross-entropy loss function

$$L = -\frac{1}{N} \sum_{i=1}^{N} \sum_{k=1}^{K} y_i^k \log \hat{y}_i^k \tag{2.2}$$

where N corresponds to the number of data points, K to the number of output neurons, $\hat{y}_i^k$ to the estimate of the model and y_i^k to the label of the ith datapoint for the kth output neuron.

Training is performed by minimizing the loss function using a form of gradient descent. For brevity, we limit ourselves to discuss Stochastic Gradient Descent (SGD), however, in recent years a multitude of alternative gradient-based optimization techniques such as ADAM [Kingma and Ba, 2015] and ADAGRAD [Duchi et al., 2011] have been proposed. SGD evaluates the derivatives

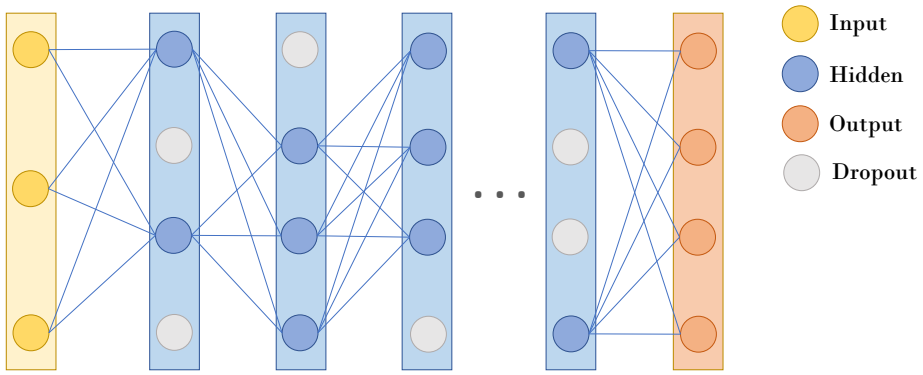

Figure 2.2: The figure displays a thinned net that might be produced during training using Dropout.

of the loss function with respect to all trainable parameters/weights in the network using backpropagation [Rumelhart et al., 1986]. Derivatives are computed based on a small subset of training data points, a batch. The weights are then updated as $w_i^{t+1} = w_i^t - \lambda \frac{\partial L}{\partial w_i^t}$, where w_i^t corresponds to the ith weight at epoch t and λ is a hyperparameter that defines how large update steps are performed in the optimization space and is referred to as the learning rate. A more detailed discussion of the training procedure is provided in [Montavon et al., 2012, Ruder, 2016].

Dropout

Dropout can be seen as a stochastic regularization technique and aims to address the overfitting issue that arises when complex models learn to fit the training data arbitrarily well but do not generalize well to unseen data. The problem is addressed by randomly dropping units (and the corresponding connections) during the training procedure, thereby preventing units from co-adapting [Srivastava et al., 2014]. However, it is not only a technique that avoids overfitting but also provides a way to combine knowledge from exponentially many neural networks in an effective way.

Dropout is performed, by temporarily dropping units at random in each layer producing a thinned network as illustrated in Figure 2.2. The probability p of dropping a given unit is chosen prior to training and is in most cases set to a default value of 0.5. However, input units generally are assigned a lower probability of being dropped. The thinned network is then trained for one weight update and the weights that remain in the network are updated. For each training sample, a new thin network is sampled and trained. This means,

that each unique network (for n units in the network there are 2^n possible networks) is rarely trained, however, training progresses since all the networks share the same set of weights.

Computing predictions from all the thin networks is infeasible at test phase, which instead averages all the prediction of the thinned networks in a single un-thinned network. This is done by scaling the learned training weights such that $W_{\text{test}}^{(l)} = pW_{\text{train}}^{(l)}$ by multiplying them with the drop-probability p.

The dropout model can be expressed as [Srivastava et al., 2014]

$$r_j^l \sim \text{Bernoulli}(p) \,, \tag{2.3}$$

$$\widetilde{\boldsymbol{y}}^l = \boldsymbol{r}^l * \boldsymbol{y}^l \,, \tag{2.4}$$

$$z_i^{l+1} = b_i^{l+1} + \sum_{j=1}^{N} w_{ij}^{l+1} \widetilde{y}_j^l \tag{2.5}$$

$$y_i^{l+1} = g(z_i^{l+1}) \,, \tag{2.6}$$

where $*$ denotes element-wise multiplication, $\boldsymbol{y}^l$ is the output and $\boldsymbol{w}^l$ and $\boldsymbol{b}^l$ are the weights and biases for layer l. $g(\cdot)$ denotes the non-linearity. As $\boldsymbol{r}^l$ is a vector of independent Bernoulli random variables with probability p of being 1, the element-wise multiplication produces the thinned outputs $\widetilde{\boldsymbol{y}}^l$.

A positive side effect of using dropout is the fact that the activations of the hidden units become sparse [Srivastava et al., 2014]. Additionally, Dropout is not only restricted to MLPs but is a general technique that can be used in most of the architectures discussed in this thesis.

2.2 Convolutional Neural Networks

Fully connected neural networks consist of a hierarchy of fully connected layers, where all units in a hidden layer are connected to all units in the previous layer. Convolutional Neural Networks (CNNs), instead, make use of convolutional layers. Thus, a CNN is a network where at least one of the fully connected layers is replaced by a convolutional layer.

The convolution operation introduces a set of assumptions that allow a considerable reduction in weight parameters. The first assumption is the fact that the units in the network are locally connected. Instead of having interactions between all units in successive layers, the convolutional operation encodes local connectivity through the filter size. These networks are therefore commonly used to process data with grid-like structure, such as time series (1D-grid),

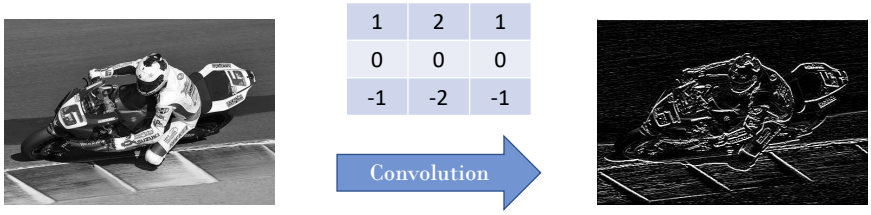

Figure 2.3: Illustration of the convolution operation. The image is convolved with the filter mask to produce the filtered image. For illustration purposes, the filter mask is chosen to be a common edge detection filter.

images (2D-grid), and videos (3D-grid). Figure 2.3 provides an example of an image that is convolved with a small convolutional filter. In convolutional neural networks, several of these filters will be learned at each layer and information will be processed in a hierarchical manner due to the stacking of multiple convolutional layers. Taking images as an example, a fully connected network would connect every pixel in the image to each neuron in the first hidden layer, convolutions instead allow the use of small filters that combine information from neighboring pixels. Here, we exploit the fact that detectors in grid-like data often only need to consider local neighborhoods. The second assumption that CNNs are based on, is the fact that the local statistics that need to be detected are invariant to location and feature detectors can, therefore, be reused at other locations in the image. This means that weight parameters can be shared across the whole image. Further, the convolutional operation introduces equivariance to translation, as translations in the input activations will lead to the same translations in output activations. Finally, an additional advantage is the fact that the convolution operation does not dependent on image size, which will become especially important for the techniques considered in Chapter 3.

For grid-like data, this reduction in parameters decreases the set of allowable functions considerable, meaning that larger networks can be learned without overfitting. For CNNs typically multiple filters are learned at each layer, where each filtering operation assuming a 2D-grid scenario, is computed as

$$y^l_{i,j} = g\left(b^l + \sum_{k=i-W/2}^{i+W/2} \sum_{m=j-W/2}^{j+W/2} w^{l-1}_{k,m} y^{l-1}_{i+k,j+m}\right), \tag{2.7}$$

where $y^l_{i,j}$ denotes the activation at spatial location (i,j) in layer l, b denotes the bias and $W \times W$ is the filter size.

Unlike traditional approaches that use fixed, pre-computed sets of filters (filter banks) [Bamberger and Smith, 1992, Leung and Malik, 2001], the advantage of

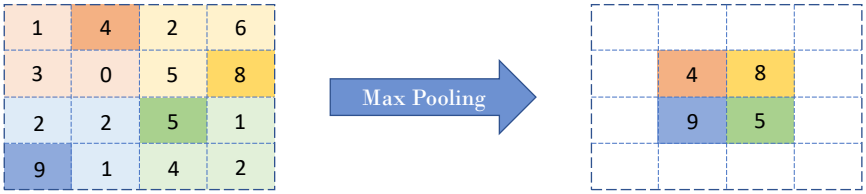

Figure 2.4: Pooling introduces invariance to small translations of the input. Here, we illustrate 2×2 max pooling (stride 2), where the image is downsampled to a fourth of the original image size and each 2×2 area in the original image is replaced with its largest value.

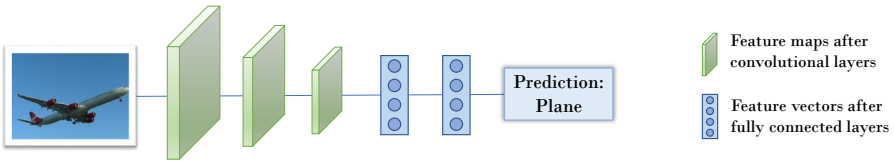

Figure 2.5: A simple convolutional neural network for a classification task. The image is processed by a set of convolutional layers (possibly interleaved with pooling operations). The final representation is then processed by fully connected layers, outputting the prediction.

CNNs is that filters are learned. This allows the learning of a useful representation for a specific problem based on data and does not require hand-designed filter banks. It has been observed that early convolutional layers still tend to learn filters similar to the traditional (hand-crafted) Gabor filters [Krizhevsky et al., 2012].

Pooling is another common operation in the context of CNNs. Pooling computes summary statistics over small local regions in the image, thereby making the feature representations (and prediction) robust to small variations in input space. Figure 2.4 provides an example of a pooling operation, where only the maximum value is kept for each 2×2 area in the image resulting in half the width and height of the original image.

Figure 2.5 illustrates an image as it is processed by a CNN for classification. The activations after the convolution (and pooling operations) are stored in feature maps of size $h \times w \times f$ where h and w are the spatial dimensions and f denotes the number of features in each layer. The convolutional layers are followed by fully connected layers in order to provide a prediction based on the features produced by the convolutional layers.

2.3 Graph Convolutional Neural Networks

In recent years, Graph Convolutional Neural Networks (GCNs) have been developed to process datasets that consist of graph structures. In many applications, it is not convenient to consider data as vectorial or grid-structured data, but instead, it is more natural to view them as graphs. Initial applications of GCNs have been among others processing of knowledge graphs, social networks, and molecules [Duvenaud et al., 2015, Kipf and Welling, 2017]. Here, we will limit the discussion to spectral GCNs that were first proposed by Bruna et al. [2014]. More recently, Defferrard et al. [2016] improved scalability, by introducing fast localized convolutions by expressing filters using Chebyshev polynomials, based on work done by Hammond et al. [2011]. Simplifications were later introduced by Kipf and Welling [2017] to further improve scalability. In this section, we will follow the notation of Kipf and Welling [2017] to briefly summarize the idea behind GCNs.

Convolutions of a signal $\boldsymbol{x} \in \mathbb{R}^N$ with a spectral filter $g_\theta = \text{diag}(\theta)$ can be expressed as a multiplication in the Fourier domain

$$g_\theta \star \boldsymbol{x} = U g_\theta U^T \boldsymbol{x} \ . \tag{2.8}$$

Here, the orthogonal matrix U corresponds to the eigenvector matrix of the normalized graph Laplacian $L = I_N - D^{-\frac{1}{2}} A D^{-\frac{1}{2}} = U \Lambda U^T$ and $U^T \boldsymbol{x}$ is the graph Fourier transform of the signal $\boldsymbol{x}$. I_N is the identity matrix, $A \in \mathbb{R}^{N \times N}$ is the adjacency matrix, $D \in \mathbb{R}^{N \times N}$ is the degree matrix, and Λ is the diagonal matrix formed from the eigenvalues of the normalized graph Laplacian. g_θ is a function of Λ. In order to avoid the eigenvalue decomposition and the costly matrix multiplications Hammond et al. [2011] showed that a truncated Chebyshev polynomial expansion of the filter $g_\theta(\Lambda)$ is a good approximation. This means that

$$g'_\theta(\Lambda) \approx \sum_{k=0}^{K} \theta'_k T_k(\tilde{\Lambda}) \ , \tag{2.9}$$

where $T_k(\tilde{\Lambda})$ denotes the Chebyshev polynomial of kth order of the scaled eigenvalues $\tilde{\Lambda} = \frac{2\Lambda}{\lambda_{\max}} - I_N$ and $\lambda_{\max}$ is the largest eigenvalue of the normalized graph Laplacian L. The Chebyshev polynomials are computed as $T_k(y) = 2yT_{k-1}(y) - T_{k-2}(y)$, with $T_0 = 1$ and $T_1 = y$. $\theta' \in \mathbb{R}^N$ are the Chebyshev coefficients.

Combining this with Equation 2.8, the spectral convolution on the graph can be defined as

$$g'_\theta \star \boldsymbol{x} \approx U \sum_{k=0}^{K} \theta'_k T_k(\tilde{\Lambda}) U^T \boldsymbol{x} \ . \tag{2.10}$$

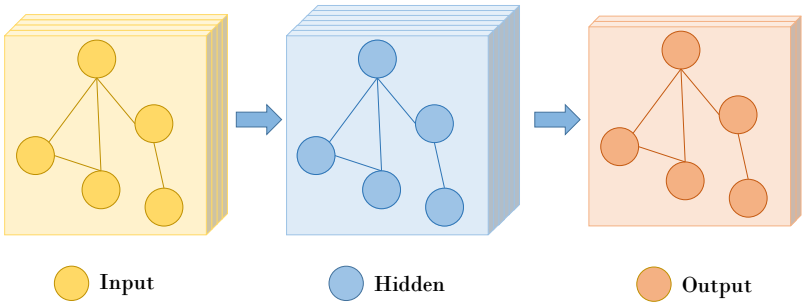

Figure 2.6: Schematic of a graph convolutional network. The input graph consists of five nodes, each represented by a four-dimensional feature vector (illustrated by the four slices in the cube). The propagation rule is applied to obtain the hidden representation. In this example, each node in the graph is represented by a six-dimensional feature vector in the hidden layer. Finally, the propagation rule is applied to produce the output.

and further

$$g'_\theta \star \boldsymbol{x} \approx \sum_{k=0}^{K} \theta'_k T_k(\tilde{L})\boldsymbol{x} \ , \tag{2.11}$$

with $\tilde{L} = \frac{2L}{\lambda_{\max}} - I_N$.

Kipf and Welling [2017] further improve scalability by adding additional simplifications, such as $K = 1$, meaning that only the $K = 1$ nearest nodes will be considered during the convolution operation. In order to propagate knowledge between distant nodes, multiple convolution operations are stacked. This is illustrated in Figure 2.6. They set $\lambda_{\max}$ as 2 and assume that the network will adapt its parameters during training to account for this value. Using the simplifications

$$g'_\theta \star \boldsymbol{x} \approx \theta'_0 \boldsymbol{x} + \theta'_1 (L - I_N)\boldsymbol{x} = \theta'_0 \boldsymbol{x} + \theta'_1 D^{-\frac{1}{2}} A D^{-\frac{1}{2}} \boldsymbol{x} \ , \tag{2.12}$$

however, to constrain the number of free parameters further and improve computational efficiency, Kipf and Welling [2017] constrain $\theta = \theta'_0 = -\theta'_1$ such that

$$g'_\theta \star \boldsymbol{x} \approx \theta (I_N + D^{-\frac{1}{2}} A D^{-\frac{1}{2}})\boldsymbol{x} \ . \tag{2.13}$$

To avoid numerical instabilities when the propagation rule is applied repeatedly due to the fact that eigenvalues of $I_N + D^{-\frac{1}{2}} A D^{-\frac{1}{2}}$ are in range $[0, 2]$, Kipf and Welling [2017] propose a renormalization by replacing $I_N + D^{-\frac{1}{2}} A D^{-\frac{1}{2}}$ with $\tilde{D}^{-\frac{1}{2}} \tilde{A} \tilde{D}^{-\frac{1}{2}}$,where $\tilde{A} = A + I_N$ and $\tilde{D}_{ii} = \sum_j \tilde{A}_{ij}$.

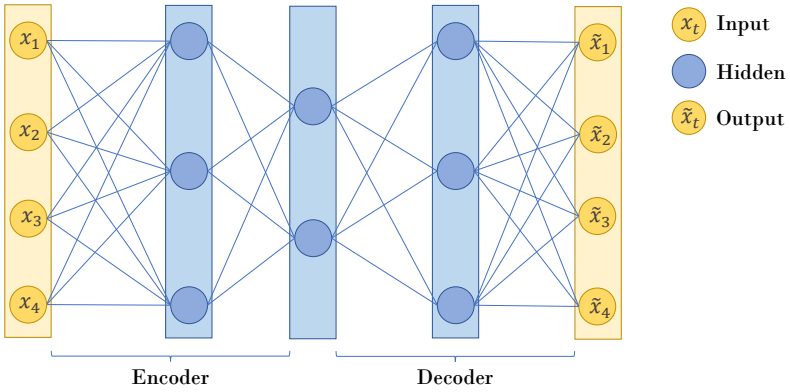

Figure 2.7: A typical AE. In this example, it consists of a two layer encoder, mapping the four dimensional input to a two dimensional code. A two layer decoder is used to map the code back to the four dimensional input space. The model is trained to reconstruct the original input.

Generalizing this to input features $X \in \mathbb{R}^{N \times C}$, with C input features per graph node, the propagation rule can be expressed as

$$Z = \sigma\left(\tilde{D}^{-\frac{1}{2}}\tilde{A}\tilde{D}^{-\frac{1}{2}}X\Theta\right) \ . \tag{2.14}$$

Here, the convolution operation is further followed by a nonlinear activation function $\sigma(\cdot)$, such as for instance $\mathrm{ReLU}(\cdot) = \max(0, \cdot)$. $\Theta \in \mathbb{R}^{C \times F}$ denotes the trainable weight matrix that remains of the polynomial filter after the simplifications. $Z \in \mathbb{R}^{N \times F}$ is used to denote the output of the graph convolutional layer with features of size F.

2.4 Autoencoders

An Autoencoder (AE) is a type of neural net, which learns a parametric map from inputs to the representation. AEs consist of two parts, an encoder f that maps the input data $\boldsymbol{x}_t$ to its representation (or code)

$$\boldsymbol{h}_t = f(\boldsymbol{x}_t; \Theta_E) \tag{2.15}$$

and a decoder g that maps the feature vector $\boldsymbol{h}_t$ back from the feature space to the input space

$$\tilde{\boldsymbol{x}}_t = g(\boldsymbol{h}_t; \Theta_D) \ . \tag{2.16}$$

The encoder and decoder functions are commonly expressed as one or more fully connected, convolutional or recurrent layers. AEs learn the parameters

Θ_E and Θ_D by optimizing the complete network for the task of reconstruction. This means that the loss function is represented by a reconstruction error, a qualitative measure of the difference between the input $\boldsymbol{x}_t$ and its reconstruction $\tilde{\boldsymbol{x}}_t$ for training example t. One natural choice of the reconstruction loss function is the Mean Square Error (MSE)

$$L_r = \frac{1}{N}\sum_{t=1}^{N}(\boldsymbol{x}_t - \tilde{\boldsymbol{x}}_t)^2 \,, \tag{2.17}$$

where N denotes the total number of training examples. Training the autoencoder to minimize the reconstruction loss can, from an information theoretic standpoint, be interpreted as maximizing the lower bound on the mutual information between the input and the codes [Vincent et al., 2010]. This is a meaningful criterion, as it ensures that as much as possible of the information in the input space is retained in the code representation.

As the aim is to learn a good representation AEs can not have a configuration where the number of hidden units is larger than the number of input (and output) units unless regularization techniques are employed. This is due to the fact that the network would be able to learn the identity function, achieving perfect reconstruction, but would not produce good representations. For non-regularized AEs, a bottleneck has historically been introduced (as seen in Figure 2.7), which forces the encoder to perform a dimensionality reduction.

AEs are closely related to more traditional dimensionality reduction techniques such as Principal Component Analysis (PCA). It has been shown that for an AE trained with a squared error objective and without non-linearities in the encoder and decoder, the AE will map data to the same subspace as obtained by PCA [Baldi and Hornik, 1989]. AE with non-linearities such as the sigmoid function can still learn the same subspace when keeping to the linear part of the non-linear function, however, they are able to learn non-linear mappings different from PCA [Japkowicz et al., 2000].

In more recent years also other approaches have emerged that introduce regularization to constrain the representation without necessarily requiring a bottleneck in the architecture. Some of the most prominent methods will be discussed in the following sections.

Denoising Auto-Encoders

One of these techniques is the Denoising Autoencoder (dAE) [Vincent et al., 2010], which changes the learning objective of the AE from reconstruction to denoising of the input. This means that given an input that is corrupted by

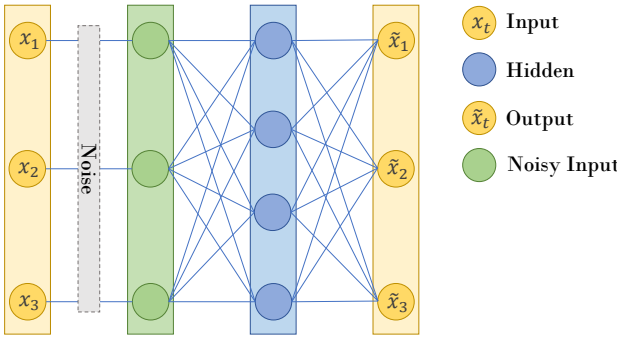

Figure 2.8: Illustration of a dAE. Noise is added to the input and the network is trained to denoise the input and produce the original clean, noise-free, input. Noise can for instance consist of masking noise (replacing inputs with 0 at random) or random Gaussian noise.

noise, the dAE is trying to reconstruct the non-corrupt input. The total loss cannot be minimized by learning the identity function, but instead, the model is forced to learn the underlying structure of the input distribution. Inputs are commonly corrupted by adding Gaussian noise, salt and pepper noise or masking noise (randomly dropping features). The modified architecture for the dAE is illustrated in Figure 2.8.

dAEs can be stacked layer-wise resulting in Stacked Denoising Autoencoders (SdAEs) [Vincent et al., 2010]. After the initial dAE is learned and an encoding function f and decoding function g are found, the encoding function can be used to train further layers. The encoding function is applied on the clean input (without added noise) to get the encoded representation. Noise is then added to the encoded representation and the training procedure for a standard dAE is performed. The process can be repeated to stack an arbitrary number of dAEs. After training, the encoding functions can be applied to the input consecutively, resulting in the final code representation. The decoding functions are applied in reverse order to produce the reconstruction.

Sparse Auto-Encoders

Another form of regularization is the Sparse Autoencoder (sAE) [Ranzato et al., 2007], which adds sparsity regularization to avoid that the model can learn the identity mapping. Sparsity regularization has been performed by penalizing the hidden biases and by directly penalizing the output of the hidden units. Approaches to penalize the hidden units directly includes the L1 penalty and

the Student-t penalty [Bengio et al., 2013].

Contractive Auto-Encoders

Contractive Autoencoders (CAEs) [Rifai et al., 2011b] are another class of AEs for learning more robust representations. The CAE adds a regularizer based on the Frobenius norm of the encoder's Jacobian $J(\boldsymbol{x})$ computed with respect to the input such that the overall loss is

$$L = \frac{1}{N}\sum_{t=1}^{N}(\boldsymbol{x}_t - \tilde{\boldsymbol{x}}_t)^2 + \lambda||J(\boldsymbol{x}_t)||_F^2 \ . \tag{2.18}$$

This penalizes the sensitivity of the features instead of solely penalizing the reconstruction error and thereby indirectly forces the reconstruction to be more robust. Additionally, this formulation has the advantage that the penalization is deterministic and not stochastic. λ controls the trade-off between reconstruction and robustness. Improved versions of the CAE exist, such as the higher order CAE [Rifai et al., 2011a].

2.5 Generative Adversarial Networks

Generative adversarial networks (GANs) [Goodfellow et al., 2014] are generative models that are trained in an adversarial manner. Unlike the discriminative models described earlier, generative models aim to estimate and represent the training data distribution. They are implicit density models, models that do not define an explicit density function but allow to sample from it. For GANs, two models are trained simultaneously, the so-called generator G that aims to generate data from a data distribution and a discriminator D, which is tasked to distinguish generated samples from the actual training data. Figure 2.9 provides a schematic illustration of this process. Training is considered a two-player minmax game, where D predicts the probability that a presented sample belongs to the training data and the generator G is trained in order to increase the probability that D makes a mistake. The generator and discriminator are commonly implemented using deep neural networks and training is performed in an end-to-end manner using backpropagation.

The generator G maps a noise variable $\boldsymbol{z}$ to the data space $G(\boldsymbol{z};\theta_g)$, where the noise distibution is represented by $p_z(\boldsymbol{z})$. The discriminator D produces a scalar for a given input $\boldsymbol{x}$. The scalar represents the probability of $\boldsymbol{x}$ being drawn from the data distribution $\boldsymbol{x}_r \sim p_{data}$ and not from the generator distribution

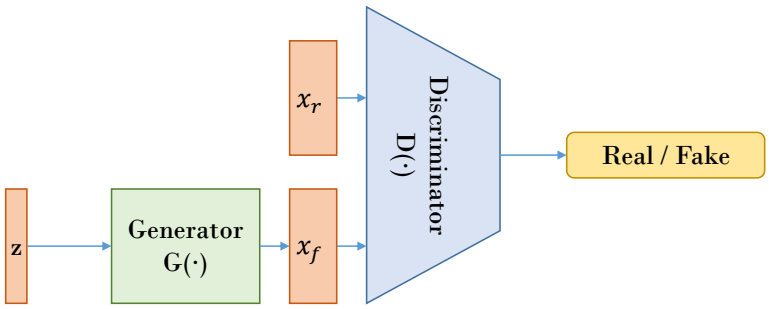

Figure 2.9: Schematic of a generative adversarial network. The generator is tasked to fool the discriminator by generating data that is close to the data distribution, while the discriminator aims aims to predict if a given input is real ($\boldsymbol{x}_r$ from the data distribution) or fake ($\boldsymbol{x}_f$ produced by the generator).

$\boldsymbol{x}_f \sim p_g$. It is parameterized as $D(\boldsymbol{x}; \theta_d)$ and the overall minmax game that is being optimized is

$$\min_G \max_D \mathcal{L}(G,D) = \mathbb{E}_{\boldsymbol{x}\sim p_{data}(\boldsymbol{x})}[\log D(\boldsymbol{x})] + \mathbb{E}_{\boldsymbol{z}\sim p_z(\boldsymbol{z})}[log(1 - D(G(\boldsymbol{z})))] \,. \tag{2.19}$$

In practice, however, due to the properties of the cross-entropy loss function, instead of training G to minimize $log(1 - D(G(\boldsymbol{z})))$, it is in practice more common to train G to maximize $log(D(G(\boldsymbol{z})))$. When minimizing the cross-entropy between a prediction and its target class, the loss will be large if the prediction is wrong, however, as the prediction is assigned to the correct class the loss will saturate. As the discriminator is minimizing the cross-entropy and the generator maximizing the same cross-entropy in the minmax formulation in Equation 2.19, the gradients for the generator will vanish if the discriminator is able to distinguish p_g samples from p_{data} samples with high certainty. Especially during early training, this can lead to problems in the training [Goodfellow, 2016].

In more recent years, many variations of the original GAN have been proposed. For instance, the deep, convolutional GAN [Radford et al., 2016], which is able to generate high-resolution images, and the Wasserstein GAN [Arjovsky et al., 2017] that adopts the Wasserstein distance in order to provide a smooth distance measure even if the probability distributions are completely disjoint.

3

Segmentation

In this chapter, we will briefly review the tasks of semantic and salient segmentation and briefly introduce some common approaches. The material discussed in this chapter builds the foundation of Papers I-IV.

3.1 Semantic Segmentation

Semantic segmentation is the task of performing pixel-wise classification in images. It is a key problem in the computer vision field for fine-grained image

Horse

Figure 3.1: From left to right, the images represent the original image (with a classification label), the ground truth for the semantic segmentation task and for the instance semantic segmentation task. Note, the instance segmentation task does not only label classes, but also distinguishes objects of the same class. All regions not assigned to a specific color are background pixels.

understanding and provides the foundation to enable tasks such as for instance self-driving cars. Figure 3.1 illustrates the difference between the classification task and the task of image segmentation. In classification one label is provided for the whole image, such as for instance Horse or Person in Figure 3.1. For the segmentation task instead, each pixel is being classified as either belonging to a specific class or as belonging to the background.

Traditionally, before the recent success of deep learning techniques, approaches have been heavily relying on the design of hand-crafted features combined with off-the-shelf classifiers such as SVMs [Fulkerson et al., 2009] and Random Forest [Shotton et al., 2008] combined with the inclusion of contextual image information [Carreira et al., 2012] and structured prediction [Carreira and Sminchisescu, 2011]. However, similarly to image classification, the main factor limiting these systems were the underlying hand-crafted features. Motivated by this, deep neural networks quickly found application in segmentation after their success on classification tasks.

Initial approaches made use of patch-based techniques, where a patch is extracted around each pixel and the pixel is classified using a CNN based on the patch [Ciresan et al., 2012, Farabet et al., 2013]. Using a sliding window approach, this allows for direct application of CNNs that have been designed for classification on the segmentation task. However, one of the drawbacks of this approach is the fact that it is computationally expensive, as patches have considerable overlap. An alternative approach is to perform superpixel segmentation and classify each superpixel using a deep neural network [Mostajabi et al., 2015]. These approaches have less of a computational overhead due to the reduced overlap, but struggle if the underlying superpixel segmentation has errors and require the conversion of the superpixels to a reasonable representation. However, using the inherent structure of CNNs, the patch-based approach can be performed more efficiently by avoiding re-computation of the features in the overlapping regions [Sermanet et al., 2014]. In order to do this, the first fully connected layer in the network is replaced by a convolutional layer, where the filter size is equal to the size of the feature map of the previous layer and the number of filters is equal to the number of neurons in the fully connected layer. All subsequent fully connected layers are replaced by 1×1 convolutions. For the fixed patch-size, these convolutional layers are equivalent to the fully connected layers. However, it allows the application of the network to larger images during the inference phase by making use of the fact that convolutions are not dependent on image size.

Current approaches make use of so-called Fully Convolutional Networks (FCNs) [Long et al., 2015a]. These are networks that do not contain fully connected layers and generally consist of an encoder that maps the image to a low-resolution representation and a decoder that produces pixel-wise

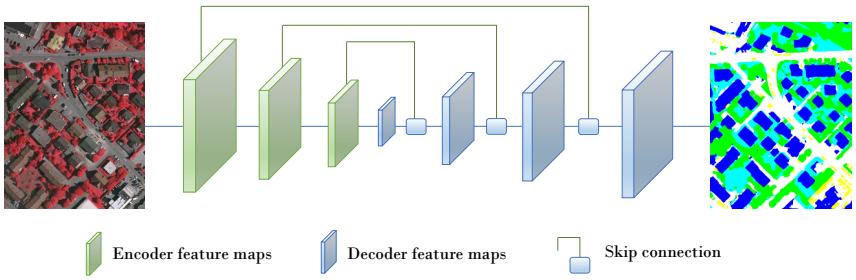

Figure 3.2: Segmentation using CNNs. These architectures consist of an encoder-decoder architecture and often include skip connections in order to use the high-resolution encoder activations to improve the upsampling and segmentation quality.

predictions. Their advantage is the fact that they are more computationally efficient, do not require a preprocessing segmentation and directly apply to whole images. Various approaches have been proposed to upsample the representation in order to produce the pixel-wise predictions from the low-resolution representation. Figure 3.2 shows such a typical segmentation architecture. For instance, Long et al. [2015a] make use of fractional strided convolutions (also referred to as deconvolutions) or bilinear interpolation in order to learn a gradual upsampling. They further introduce skip connections, where high-resolution information from the early layers in the encoder is used to improve segmentation details. Segnet [Badrinarayanan et al., 2015] instead makes use of a symmetric architecture, where pooling indices from the encoder are stored and activations in the decoder are upsampled by placing them in the locations corresponding to the indices. The sparse activations after 'unpooling' are then processed and made dense by additional convolution operations. Other more recent advances include for instance DeepLab [Chen et al., 2018, 2017], which makes use of among others, atrous convolutions. Atrous convolutions can be used to provide filters with a larger field of view to enable them to integrate more context. Their advantage is that they do not add additional parameters compared to a common convolution filter of equivalent size.

Recently, the task of semantic segmentation has been refined to not only segment out different classes but further distinguish different objects from the same class. Figure 3.1 illustrates the difference between traditional semantic segmentation and instance-level semantic segmentation. Initial attempts approached the problem of instance segmentation by first proposing segmentation proposals and then classify them using object detection networks [Dai et al., 2016a, Pinheiro et al., 2015]. Alternatively, object detection is performed

Figure 3.3: From left to right, the images represent the original image and the ground truth for the salient segmentation and the instance salient segmentation tasks.

and based on the bounding box proposals, the objects are segmented [Dai et al., 2016b]. A recent state-of-the-art approach, where object detection and segment proposal is done in parallel, is Mask-RCNN [He et al., 2017]. Mask-RCNN performs segmentation by extending Faster-RCNN [Ren et al., 2015], an object detection network. Faster-RCNN consists of a two-stage architecture. The first stage consists of a so-called Region Proposal Network, which is trained to predict bounding boxes for candidate regions. The second stage extracts features for each proposal region and performs classification and bounding box regression. Mask-RCNN performs instance-level segmentation by adding a segmentation branch that outputs a mask for each prediction in parallel to the existing bounding box regression and class prediction branches.

3.2 Salient Segmentation

Salient segmentation is similar to semantic segmentation, however, it does not rely on class information and instead aims to segment attention-grabbing objects in the image, i.e. objects that stand out due to their contrast with respect to surrounding areas. It is a fundamental task in computer vision and is often used as a pre-processing technique to enable other tasks, such as face detection [Liu et al., 2017], video summarization [Ma et al., 2002], and object detection [Navalpakkam and Itti, 2006]. Figure 3.3 illustrates the task of salient segmentation.

Similar to the task of semantic segmentation, traditional approaches have to a large extent relied on hand-crafted features. Common features include low-level information such as contrast, changes in color, intensity, texture [Cheng et al., 2015, Liu et al., 2011, Perazzi et al., 2012, Valenti et al., 2009] or frequency information [Achanta et al., 2009]. However, designing robust hand-crafted features that generalize well to a wide range of scenarios is challenging, which led to the use of representation learning techniques and more specifically deep learning approaches. For instance, Li and Yu [2015] propose the use of convo-

lutional neural networks to extract feature representations at multiple scales for a given region in the image and fuse them to produce the salient prediction for the image region. Wang et al. [2015] approach the task from a patch-based approach and use CNNs to extract features for a center pixel based on the local surrounding area. Object proposals are then used to refine the salient prediction. In recent years, FCNs have also been used for salient segmentation. Li and Yu [2016] make use of a two-stream approach where one stream consists of a multi-scale FCN providing pixel-level segmentation results and combine it with a second stream that provides segmentation results on a superpixel level. Predictions are fused using an additional convolution operation in order to obtain the final salient segmentation. Li et al. [2017] makes use of a multi-scale FCN and utilizes attention weights to fuse the multiple scales.

Inspired by the research on the instance segmentation task, the task of instance salient segmentation was proposed by Li et al. [2017]. It aims to not only segment salient regions but further aims to distinguish individual salient objects. Using their multi-scale FCN with attention weights, they produce both a salient segmentation and object contours. The object contours are used to produce salient instance proposal by first generating proposals using multiscale combinatorial grouping [Arbeláez et al., 2014] and then making use of a MAP-based subset optimization framework [Zhang et al., 2016] in order to filter the number of proposals and produce a compact set. Finally, a fully connected conditional random field is applied to refine the segmentation results. Note, that this task is closely related to and can be considered a sub-task of instance segmentation in the sense that different instances need to be separated. However, no class information needs to be predicted for instance salient segmentation.

4

Unsupervised Learning

Unsupervised learning aims to describe unlabeled data by exploiting the statistical structure of the data. This chapter provides background on the unsupervised tasks considered in this thesis. Namely, we consider unsupervised domain adaptation in order to support Paper III, representation learning for Paper V, clustering for Paper VI, and finally zero-shot learning for Paper VII.

4.1 Domain Adaptation

Domain adaptation addresses the problem of domain shift [Gretton et al., 2009] in machine learning. Domain shift is a phenomena that is often encountered in machine learning and arises from the fact that training data $D_{tr} = \{(\boldsymbol{x}_i^{tr}, y_i^{tr})\ i = 1, ..., N\}$, where $\boldsymbol{x}_i^{tr}, y_i^{tr}$ are feature vector and label pairs, might come from a probability distribution $P_{tr}(x, y)$, while test data $D_{te} = \{(\boldsymbol{x}_i^{te}, y_i^{te})\ i = 1, ..., N\}$ come from a different distribution $P_{te}(x, y)$. The training domain is commonly referred to as the source domain, while the testing domain is referred to as the target. This can, for instance, be encountered when satellite images are taken in different countries, where buildings exhibit considerable differences, or with images that have been acquired using separate imaging protocols or sensors. Further, there has been increasing interest in utilizing synthetic data for among others, the task of self-driving cars [Johnson-Roberson et al., 2017]. Domain adaptation can be used to enable the use of models that have been trained on synthetic data on real data.

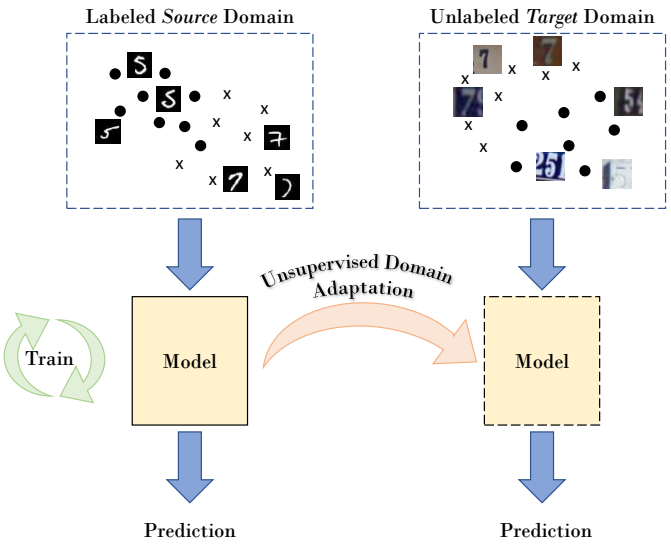

Figure 4.1: Illustration of the unsupervised domain adaptation task. Given a labeled source domain, a model can be trained for a given prediction task. However, for unsupervised domain adaptation, we further have an unlabeled target domain that contains the same classes. Unsupervised domain adaptation aims to adapt the source model to predict in the target domain.

In deep learning, this problem has often be addressed by collecting additional data and making use of transfer learning techniques to finetune the model on data from the new distribution. However, this is not always feasible as data in certain domains, such as for instance the medical domain, are expensive to obtain. Unsupervised domain adaptation approaches instead aim to find a remedy to the scenario when no labels are available for the target domain. The task of unsupervised domain adaptation is depicted in Figure 4.1. The problem has been approached by mapping source and target representations into a joint feature space by minimizing the maximum mean discrepancy between features [Long et al., 2015b, Tzeng et al., 2014]. More recently, adversarial approaches have found application on the task and these are the ones most relevant for this thesis. Tzeng et al. [2017] introduced a generalized framework for adversarial domain adaptation, where existing adversarial approaches have been categorized according to three different properties. The first one is the type of base model that is used to produce a feature representation based on the source and target inputs, namely is it a generative or discriminative model. The second criterion is whether or not the weights of these base models are shared for both domains and finally, what type of loss has been used. Based on the framework a new model called adversarial discriminative domain adaptation (ADDA) is proposed that makes use of a discriminative base model, unshared

weights, and a generative adversarial loss function [Tzeng et al., 2017].

In ADDA, a CNN is first trained to classify source domain images. Once the network has been trained, the feature extraction part of the network is separated from the classifier, the weights are frozen, and a discriminative loss is optimized between features for the source domain and features of a feature extraction network on the target domain. The discriminator is trained to distinguish features from the source and target domain, forcing the target feature extraction network to produce features for the target domain that are similar to the features for the source domain, effectively aligning the features. During testing, the feature extraction network that has been trained for the target domain is combined with the classifier that was trained on top of the source feature extraction network.

In Paper III, we propose a new adversarial approach that aims to learn the feature extraction and the classifier jointly, apply it for the task of medical image semantic segmentation, and compare its performance to ADDA.

4.2 Representation Learning

Representation learning is the process of learning *meaningful* representations from data [Bengio et al., 2013] and aims to replace the necessity of hand-crafted feature design. Hand-crafting of features is a labor-intensive and cumbersome process that is often very application specific making it difficult to design good robust features. However, good representations can have a huge impact on further processing, such as for example for the training of classifiers and clustering. By instead learning feature representations from data machine learning approaches can be made less reliant on feature design and learning approaches can be made more robust.

Representation learning has found application in a wide range of domains, such as image classification [Hinton et al., 2006], object detection [Ren et al., 2017], speech recognition [Dahl et al., 2010] and methods to produce word embeddings [Mikolov et al., 2013]. In this section, we will restrict the discussion mainly to unsupervised deep learning approaches. In the literature, many assumptions have been proposed on what a *meaningful* representation consists of. For instance, sparsity priors have been used in order to ensure that sparse representations are encouraged where observations are only represented by a small set of features. Sparse autoencoders as discussed in Chapter 2.4 are an example of such a method and other approaches include sparse coding [Olshausen and Field, 1996]. Other common priors that have been used are that representations should be robust to noise (i.e. denoising autoencoders [Vincent et al., 2010])

and robust to small input variations (i.e. contractive autoencoders [Rifai et al., 2011b]).

Beside non-probabilistic approaches such as autoencoders (discussed in Chapter 2.4), probabilistic approaches also exist. One of the most prominent approaches has been the Restricted Boltzmann Machine (RBM) [Hinton, 2010, Smolensky, 1986]. RBMs are a restricted type of Boltzmann Machine (BM), which is a class of energy based models and can be viewed as two-layer stochastic, energy-based neural networks that attempt to fit a probability distribution to the training data. They consist of a layer of visible (input) units that represent the components of an observation, and a layer of hidden units that models dependencies between the various observations. The units in the hidden layer correspond to stochastic binary feature detectors, whereas the visible units represent the observed binary states. Unlike in a standard neural network, connections between units are undirected and all units are connected to each other. Inference is, however, due to the inter-layer connections, intractable for most scenarios, as computing the conditional probability of visible and hidden units requires marginalizing over the rest of the hidden or visible units, respectively. Adding restrictions to the BM interaction pattern leads to a new model, the RBM, where all of the units in the hidden and visible layer are connected with no intra-layer connections to form a complete bipartite graph. Applications include collaborative filtering [Salakhutdinov et al., 2007], image generation [Hinton et al., 2006], and speech recognition [Dahl et al., 2010]. For a more detailed discussion of RBMs, the interested reader is referred to Bengio et al. [2013].

Recently, VAEs [Kingma and Welling, 2014], another probabilistic approach has been proposed. Similar to deterministic autoencoders, these models consist of an encoder and a decoder. However, unlike in the case of deterministic autoencoders, which produces a deterministic latent representation, the encoder in a VAE produces parameters for the distribution that generates the latent representation (typically a Multivariate Gaussian distribution). For simplicity it is common to assume a diagonal covariance structure. Given the mean and the variance of the distribution, a latent representation is sampled from the distribution and passed to the decoder, which generates a data point, which, in a trained model, is close to the original input of the autoencoder. The model is optimized by maximizing the Evidence Lower Bound using stochastic gradient descent. A detailed discussion of this is out of scope for this thesis and the interested reader is referred to Kingma and Welling [2014].

4.3 Clustering

The process of discovering the underlying structure of data in order to group data into compact groups, separated from each other, is referred to as clustering. Due to large amounts of available unlabeled data, the field of clustering has found application for various tasks. For instance, applications include outlier detection [Hodge and Austin, 2004], collaborative filtering [Ungar and Foster, 1998], pose estimation [Shotton et al., 2011], topic discovery [Sahami and Koller, 1998] and sequence analysis in computational biology [Eisen et al., 1998].

Concretely, clustering is the task of finding the underlying K groups, provided feature representations $\mathcal{X}_{tr} = \{\boldsymbol{X}_i \; i = 1, ..., N\}$ of N data points, based on a measure of similarity [Jain, 2010]. The objective is to achieve groupings, where the underlying groups have high intra-group similarity and low inter-group similarity. The focus in the clustering field is on how to find meaningful similarities that allow the discovery of sensible clusters in an unsupervised manner.

Clustering and the development of clustering methodology has been an active field of research for decades [Sokal, 1963]. The various approaches to clustering can be divided into two main categories, hierarchical and partitional clustering algorithms. The two different approaches are illustrated in Figure 4.2. Hierarchical approaches are designed to find clusters in a recursive manner and either i) start by considering each data point as a separate cluster and recursively joining the most similar clusters together (agglomerative hierarchical clustering) or ii) by initially considering all data points as a single cluster and recursively divide clusters (divisive hierarchical clustering) [Jain, 2010]. This results in a hierarchical structure of clusters. Partitional clustering instead, the clustering performed in this thesis in Paper VI, assigns data points to clusters without the assumption of hierarchical structure.

A vast number of partitional clustering approaches exist, with some of the most common approaches being k-means [MacQueen, 1967], mean-shift [Comaniciu and Meer, 2002] and expectation maximization based clustering approaches [Dempster et al., 1977]. However, in order for these algorithms to succeed it is important to represent data in a way that allows the definition of meaningful similarity metrics. For complex images, for instance, it will not be meaningful to only consider the RGB-values of the pixels directly as data representations for clustering methods such as k-means, as images that contain identical objects but at different locations will exhibit large differences. Instead, it is important to define a meaningful feature space as well as a meaningful distance in this space. Previous work has mainly focused on the distance metric and to a large extent considered the feature design application-specific.

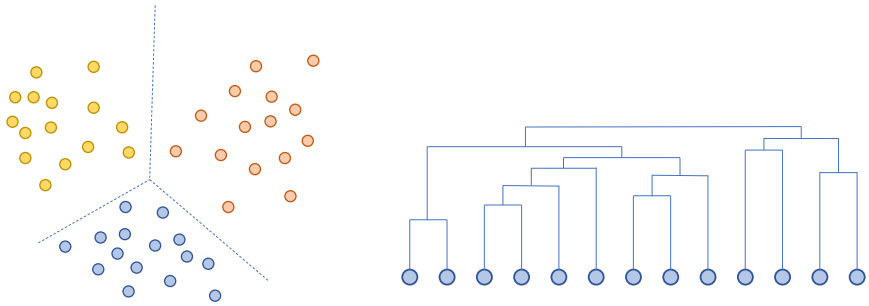

Figure 4.2: Left: Points are assinged directly to clusters in a non-hierarchical structure (partitional clustering). Right: Points are clustered in an hierarchical manner (hierarchical clustering).

Recently, approaches have been developed for the use of clustering that attempt to learn the data representation (representation learning as discussed in the previous section) as well as the clustering assignment. For instance, Tian et al. [2014] draws parallels between autoencoders and spectral clustering and makes use of autoencoders to learn representations before performing k-means clustering. Another such approach that inspired our work in Paper VI is DEC [Xie et al., 2016]. DEC learns the feature representation and the cluster assignments and the feature representation simultaneously in an alternating training procedure. Given a mapping function in form of a deep neural network and a set of initial cluster centers, the first step is based on the soft cluster assignment of data points to cluster centers. The second step then relies on updating the parameters of the neural network as well as the cluster centers in order to match the soft assignments to a pre-defined target distribution which encourages cluster purity but also assigns higher importance to points that are assigned to a certain cluster with high confidence. In order to facilitate this training procedure, DEC needs good initialization of the network and therefore requires pretraining of the neural network. In Paper VI, we instead propose a new approach that aims to reduce the need for pretraining.

4.4 Zero-shot Learning

The task of zero-shot learning, or zero-shot classification, considers the task of predicting the correct class labels for data points, without previously seeing examples for these classes during training. In order to do this, relations between the classes that were seen during training and the unseen classes are exploited based on meta-information. This can, for instance, include handcrafted attributes for each class [Akata et al., 2013, Li et al., 2018b, Parikh and

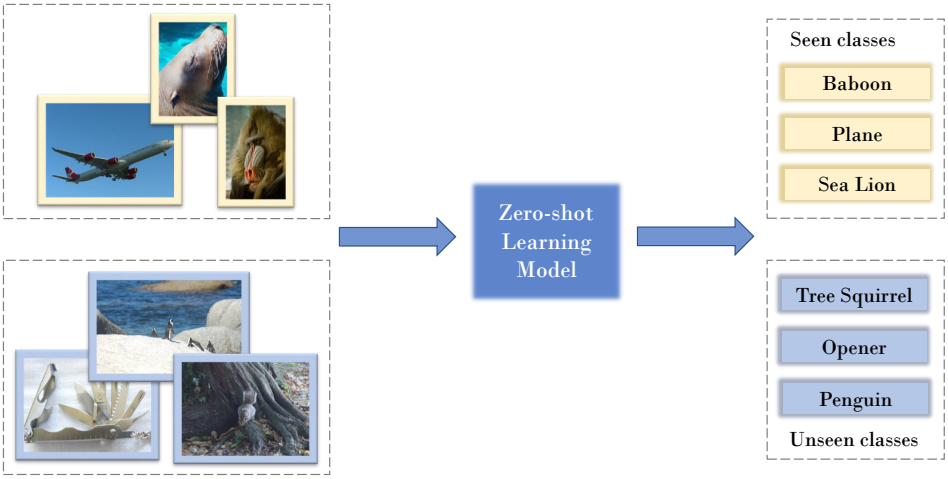

Figure 4.3: Zero-shot learning task aims to use semantic class information to allow the prediction of images to previously unseen classes or a mix of seen and unseen classes. Note, test and training classes are completely disjoint.

Grauman, 2011], but can also be more general, and arguably unsupervised when based on more general class-information such as the word embedding of a class name [Frome et al., 2013, Norouzi et al., 2014] or a knowledge graph [Wang et al., 2018]. The necessity for methods to extend to previously unseen classes can arise for example in situations such as marketing, where new products are continuously designed and introduced, or in medical imaging where labeled data examples are sparse and might not be available for some classes. The task of zero-shot learning is depicted in Figure 4.3.

More concretely, we can define the task of zero-shot classification as assigning test data samples to previously unseen classes C_{te} based on the availability of a L dimensional semantic representation vector $z \in \mathbb{R}^L$ per class C. Here, C_{te} denotes the set of all test classes. Further, labeled training data $D_{tr} = \{(X_i, c_i)\, i = 1, ..., N\}$ exists for the training classes C_{tr}, where X_i denotes the ith training sample and $c_i \in C_{tr}$ the corresponding class label. C_{tr} corresponds to the set of all training classes. Unlike in the supervised classification scenario, the test and training classes are completely disjoint $C_{te} \cap C_{tr} = \emptyset$.

Zero-shot learning has been explored in an extensive set of works recently. We separate them into two main groups based on the type of meta-information that is being used, namely semantic information such as hand-crafted attributes for each class or word embeddings of class names, and approaches based on meta-information in form of knowledge graphs. The former approaches generally either align the semantic information and the image information in a joint embedding space [Akata et al., 2015, Romera-Paredes and Torr, 2015], align the

image information with the semantic information in the semantic space [Frome et al., 2013, Socher et al., 2013] or align the semantic information with the image information in the image space [Zhang et al., 2017]. In the inference phase distance metrics are applied in these spaces to find the closest class representation to a given image.

Approaches that use knowledge graphs are less explored and are based on the assumption that the unseen classes can exploit the similarity to the seen classes in the graph. One such recent approach, which can also be considered a hybrid approach as it makes use of both semantic information and the knowledge graph was proposed by Wang et al. [2018]. In this work, a GCN is trained to predict a set of logistic regression classifiers on top of pretrained CNN features.

In Paper VII, we revisit the use of GCNs for the task of zero-shot learning and propose an efficient knowledge graph propagation procedure that allows us to improve on previous approaches.

5

Kernel Methods and Information Theoretic Learning

The material presented in this section will mainly provide the foundations for the work presented in Paper V and Paper VI. We will first review the underlying ideas of kernel methods and then briefly outline some of the concepts in Information Theoretic Learning.

5.1 Kernel Methods

Kernel methods aim to model non-linear structure in data, while at the same time building on the well-understood theory of linear methods. This is achieved by making use of Mercer kernels to implicitly map data points into a high-dimensional and possible infinite reproducing kernel Hilbert space (RKHS). In the high dimensional space, data points are likely to be linear separable [Cover and Thomas, 1991] and linear methods can be applied. In order to do this, the so-called kernel trick is applied by expressing the operations in the kernel space through inner products. In this way, the explicit mapping $\phi(\cdot)$ to the kernel space does not need to be computed, but instead, a kernel is used to directly compute these inner products. A kernel $K(\cdot,\cdot)$ is a function that computes inner products

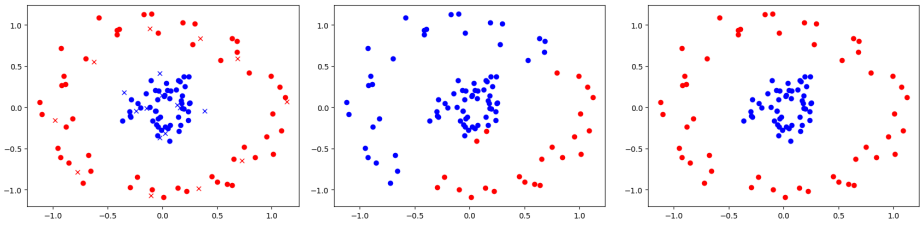

Dataset **Linear SVM** **Kernel SVM**

Figure 5.1: The simple dataset on the left contains two classes (red and blue) and consists of a training set (represented by crosses) and a test set (represented by circles). The linear SVM struggles to classify the test dataset correctly due to the fact that it is restricted to modeling a linear decision plane. Utilizing the ideas of kernel methods, the kernel SVM instead is able to classify the data points correctly. Here an RBF kernel is used.

in the high dimensional space such that

$$K(\boldsymbol{x}_i, \boldsymbol{x}_j) = \langle \phi(\boldsymbol{x}_i), \phi(\boldsymbol{x}_j) \rangle \,, \tag{5.1}$$

where $\phi(\cdot)$ corresponds to the mapping to the potentially high dimensional feature space and $\langle \cdot, \cdot \rangle$ denotes the inner product operator.

According to Mercer's Theorem [Mercer, 1909, Shawe-Taylor and Cristianini, 2004], we know that for a symmetric continous function $K(\boldsymbol{x}, \boldsymbol{z})$ that satisfies

$$\int \int K(\boldsymbol{x}, \boldsymbol{z}) g(\boldsymbol{x}) g(\boldsymbol{z}) \partial \boldsymbol{x} \partial \boldsymbol{z} \geq 0 \tag{5.2}$$

for all $\boldsymbol{x}, \boldsymbol{z} \in \mathbb{R}^d$ and for all square integrable functions $g(\cdot)$, there exists a space where $K(\boldsymbol{x}, \boldsymbol{y})$ defines an inner product such that Equation 5.1 holds for some mapping $\phi(\cdot)$.

This has been heavily exploited in the past three decades by replacing inner product computations in traditional linear methods such as SVMs and PCA with kernel functions. Figure 5.1 shows a simple dataset that is not linearly separable and illustrates how a linear SVM and a kernel SVM perform on it. The kernel SVMs ability to express non-linear decision planes allows it to classify points correctly, while the linear SVM is not able to classify points correctly.

5.2 Information Theoretic Learning

Traditionally, most approaches to learning adaptive systems have been addressed using second-order statistics, such as for instance the MSE criteria. These criteria perform well for the learning of linear models and many non-linear models, however, it can be beneficial to consider higher-order statistical properties of the underlying processes, especially for tasks such as manifold learning, classification, and clustering [Jenssen et al., 2006]. Information theoretic learning aims to do this by making use of information theoretic objective functions. One important aspect of information theoretic learning is to define and measure similarity and dissimilarity between PDFs. One of the most known and used divergence measures is the Kullback-Leibler (KL) divergence, which for continuous random variables is

$$D_{KL}(p||q) = \int_X p(\boldsymbol{x}) \log \frac{p(\boldsymbol{x})}{q(\boldsymbol{x})} \partial x \tag{5.3}$$

and for discrete probability distributions is

$$D_{KL}(p||q) = \sum_x p(\boldsymbol{x}) \log \frac{p(\boldsymbol{x})}{q(\boldsymbol{x})} \ . \tag{5.4}$$

The KL-divergence is also sometimes referred to as information gain and represents the information that is gained if the original distribution p is used instead of the approximating distribution q. It measures the dissimilarity between the probability distributions p and q. Note, the minimum of D_{KL} is 0 and obtained if and only if $q = p$, however, it is not a metric as it is not symmetric and does not adhere to the triangle inequality. Symmetric versions of the KL-divergence exist. For instance, the symmetric Jeffrey (J) divergence [Principe, 2010]

$$D_J(p||q) = \sqrt{\frac{1}{2}(D_{KL}(p||q))^2 + \frac{1}{2}(D_{KL}(q||p))^2}. \tag{5.5}$$

5.2.1 Cauchy-Schwartz Divergence

Another divergence and the underlying divergence used in Paper VI is the Cauchy-Schwartz (CS) divergence. We first present the CS-divergence, before

briefly discussing Parzen kernel density estimation, a non-parametric density estimation technique, which is used in Paper VI to derive an estimator for the CS-divergence. Finally, we conclude the section by outlining how the estimator can be obtained as presented in Jenssen et al. [2006].

The CS-divergence's name originates from the CS-inequality, which states that

$$\|\boldsymbol{x}\|^2\|\boldsymbol{y}\|^2 \geq (\boldsymbol{x}^T\boldsymbol{y})^2 \tag{5.6}$$

such that

$$-\log \frac{(\boldsymbol{x}^T\boldsymbol{y})}{\sqrt{\|\boldsymbol{x}\|^2\|\boldsymbol{y}\|^2}} \geq 0 \ . \tag{5.7}$$

Based on this inequality, Principe and Xu [2000] defined the CS-divergence measure as

$$D_{CS}(p\|q) = -\frac{\int p(\boldsymbol{x})q(\boldsymbol{x})\partial\boldsymbol{x}}{\sqrt{\int p^2(\boldsymbol{x})\partial\boldsymbol{x} \int q^2(\boldsymbol{x})\partial\boldsymbol{x}}} \ . \tag{5.8}$$

From the CS-inequality, we know that this formulation ensures non-negativity and it will only be 0 if and only if $p(\boldsymbol{x}) = q(\boldsymbol{x})$. Similar to the KL-divergence, the CS-divergence does not adhere to the triangle inequality, however, it is symmetric. In Paper VI, this cost function is utilized to perform clustering by ensuring that clusters are compact and separated, a natural objective of clustering. Given two clusters, we can represent each cluster by a PDF. By maximizing the above formulation, we can see that compactness and separation are inherently represented. In order to maximize the expressions, the denominator has to be large, and samples within each of the given clusters must, therefore, be highly similar. Similarly, the nominator should be small, which is achieved when the similarity between samples across clusters is small.

Parzen kernel density estimation

Parzen kernel density estimation is a non-parametric density estimation technique. Unlike in the case of parametric density estimation, non-parametric techniques do not require a priori assumptions on the parametric model for the PDF and are therefore ideal in a situation where the underlying model is unknown. Given a set of N data points $\boldsymbol{x}_1, \ldots, \boldsymbol{x}_N$ the density $\hat{p}(\boldsymbol{x})$ can be estimated using the Parzen kernel density estimator

$$\hat{p}(\boldsymbol{x}) = \frac{1}{N}\sum_{i=1}^{N} W_{\sigma^2}(\boldsymbol{x}, \boldsymbol{x}_i) \ , \tag{5.9}$$

where W_{σ^2} is used to denote the Parzen kernel, which itself has to integrate to one. Note that this also links to the kernel methods discussed in Chapter 5, as the density in a point can be viewed as the mean of the inner products between that point and the other datapoints in kernel space. The most common choice of kernel is the Gaussian kernel

$$W_{\sigma^2}(\boldsymbol{x}, \boldsymbol{x}_i) = \frac{1}{(2\pi\sigma^2)^{d/2}} e^{-\frac{\|\boldsymbol{x}-\boldsymbol{x}_i\|^2}{2\sigma^2}} . \tag{5.10}$$

σ is a hyperparameter representing the width of the the kernel and has a large effect on the estimate. Small σ values generally result in very local spikes that do not represent the underlying distribution well, while large values lead to overly smooth estimated distributions.

Estimation of Cauchy-Schwartz Divergence

The estimator discussed in this section was initially proposed in Jenssen et al. [2006]. In order to estimate the CS-divergence, a parzen kernel density estimate is used for the two densities p and q in Equation 5.8. From Equation 5.9, we have

$$\hat{p}(\boldsymbol{x}) = \frac{1}{N_1} \sum_{i=1}^{N_1} W_{\sigma^2}(\boldsymbol{x}, \boldsymbol{x}_i) \ , \ \hat{q}(\boldsymbol{x}) = \frac{1}{N_2} \sum_{j=1}^{N_2} W_{\sigma^2}(\boldsymbol{x}, \boldsymbol{x}_j) \ . \tag{5.11}$$

Further, we can make use of the fact that the convolution of two Gaussian functions is a Gaussian with a variance corresponding to the sum of the variances of the individual Gaussians. Thus, we have

$$\int W_{\sigma^2}(\boldsymbol{x}, \boldsymbol{x}_i) W_{\sigma^2}(\boldsymbol{x}, \boldsymbol{x}_j) \partial \boldsymbol{x} = W_{2\sigma^2}(\boldsymbol{x}_i, \boldsymbol{x}_j) \ . \tag{5.12}$$

Making use of this relation and the parzen estimators for p and q we can express the nominator in Equation 5.8 as

$$\int p(\boldsymbol{x}) q(\boldsymbol{x}) \partial x \approx \int \hat{p}(\boldsymbol{x}) \hat{q}(\boldsymbol{x}) \partial x \tag{5.13}$$

$$= \frac{1}{N_1 N_2} \sum_{i,j=1}^{N_1, N_2} W_{2\sigma^2}(\boldsymbol{x}_i, \boldsymbol{x}_j) \tag{5.14}$$

$$= \frac{1}{N_1 N_2} \sum_{i,j=1}^{N_1, N_2} k_{ij} \ . \tag{5.15}$$

Here, we use k_{ij} to denote $W_{2\sigma^2}(\boldsymbol{x}_i, \boldsymbol{x}_j)$. Similar we can express the denominator, such that the estimator for the CS-divergence is given as

$$\hat{D}_{CS}(p\|q) = -\log \frac{\sum_{i,j=1}^{N_1,N_2} k_{ij}}{\sqrt{\sum_{i,i'=1}^{N_1,N_1} k_{ii'} \sum_{j,j'=1}^{N_2,N_2} k_{jj'}}} \,. \tag{5.16}$$

Part II

Summary of research

6

Paper I

Semantic Segmentation of Small Objects and Modeling of Uncertainty in Urban Remote Sensing Images Using Deep Convolutional Neural Networks

Michael Kampffmeyer, Arnt-Børre Salberg, and Robert Jenssen

Proceedings of the IEEE Conference on Computer Vision and Pattern Recognition Workshops 2016

This paper explores the use of CNNs for the task of urban land cover segmentation and addresses the challenge of class-imbalance by the use of a loss function that balances the loss according to the class frequency. Given airborne images and digital surface models, we design and learn a model that is able to segment the image into a set of different classes, namely buildings, trees, low-vegetation, roads, and cars. We further perform a comparison of two approaches to the task of segmentation, namely patch-based pixel classification and a more recent end-to-end learnable approach of using a FCN architecture (see Figure 6.1). We illustrate that the end-to-end approach consistently outperforms the patch-based approach. Finally, the paper presents an evaluation of model uncertainty in the context of urban land-cover classification by integrating advances from Bayesian neural networks and we conclude that it is a good measure for pixel-wise uncertainty in remote sensing.

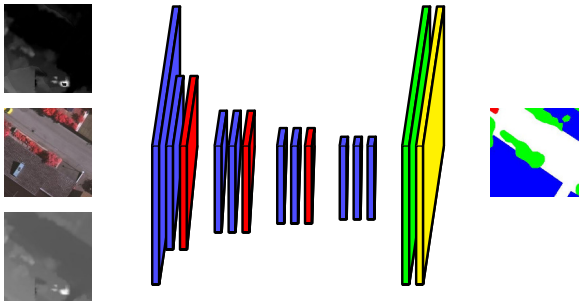

Figure 6.1: FCN network used in Paper I. Input modalities consist of airborne images, a digital surface model and a normalized digital surface model.

Contributions by the author

- The idea was developed in a joint collaboration with Arnt-Børre Salberg and Robert Jenssen.
- I implemented the proposed models and performed the experiments.
- I wrote the manuscript draft of the paper.

7

Paper II

Urban Land Cover Classification with Missing Data Modalities Using Deep Convolutional Neural Networks

Michael Kampffmeyer, Arnt-Børre Salberg, and Robert Jenssen

Journal of Selected Topics in Applied Earth Observations and Remote Sensing, 2018

This paper is a direct successor of Paper I. In this work, we continue the exploration of CNNs for urban land cover classification. Especially we focus in this paper on the problem of missing data modalities. Fusing different data modalities is a common approach in remote sensing to improve model performance. For instance, in Paper I we made use of digital surface models in addition to airborne images. However, this raises the question of what happens if some data modalities are missing during the inference stage. The naïve approach to this problem would be to train separate models for the individual modality pairs, however, in this case, a large amount of information is being ignored during the inference phase. Instead, based on recent works by Hoffman et al. [2016] we introduce Hallucination Networks to the task of urban land cover segmentation. These models allow the use of all available training modalities by learning mappings from one data modality to the feature representation of a potentially missing data modality. We further investigate the scenarios of partly missing data modalities and the scenario where multiple data modalities are missing. Figure 7.1 illustrates the issue addressed in this work. Our

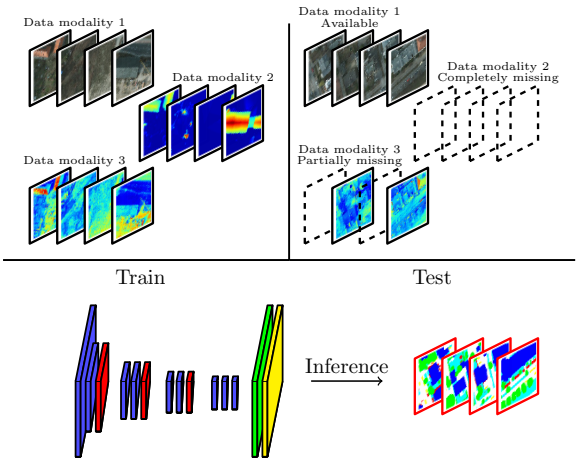

Figure 7.1: Concept figure illustrating the issue addressed in this paper. We propose a method to produce urban land cover classification when some data modalities are missing partially or completely during the test phase. The top part of the figure illustrates a scenario, where data modality 2 is completely missing during testing and modality 3 is missing for some of the test images. We leverage all available training modalities (top left part of the figure) to increase overall performance when performing inference (bottom part of figure).

empirical results show that the proposed models outperform models trained only on the available data modalities, as well as ensemble models trained only on the available modalities. This makes them an attractive choice for handling missing data modalities in urban land cover classification.

Contributions by the author

- The idea was conceived by me and developed in collaboration with Arnt-Børre Salberg and Robert Jenssen.
- I implemented the proposed models and performed the experiments.
- I wrote the manuscript draft of the paper.

8

Paper III

Unsupervised Domain Adaptation for Automatic Estimation of Cardiothoracic Ratio

Nanqing Dong, Michael Kampffmeyer, Xiaodan Liang, Zeya Wang, Wei Dai, Eric P. Xing

Proceedings of the International Conference on Medical Image Computing and Computer Assisted Intervention 2018

The medical domain is notorious for the limited availability of data due to privacy concerns and the cost of getting medical experts to provide labels. A common approach to learn in the presence of limited data is the use of finetuning, i.e. training models on large available (possibly unrelated) datasets and finetune the model on the task of interest. However, this requires a set of labels for the new dataset, which may not be available. A naïve approach would be to train the model on available datasets that have been obtained by different hospitals, however, as these images are generally produced with different image protocols, they contain different noise levels and varying contrast.

The paper approaches this problem from an unsupervised domain adaptation perspective. We propose a framework that builds on our intuition that the segmentation prediction masks should be domain independent and train the framework in an adversarial manner, utilizing a discriminator that aims to distinguish the segmentation prediction mask from the ground truth mask. The framework is illustrated in Figure 8.1. This allows us to perform segmentation on an unlabeled dataset based on an openly available dataset in order to

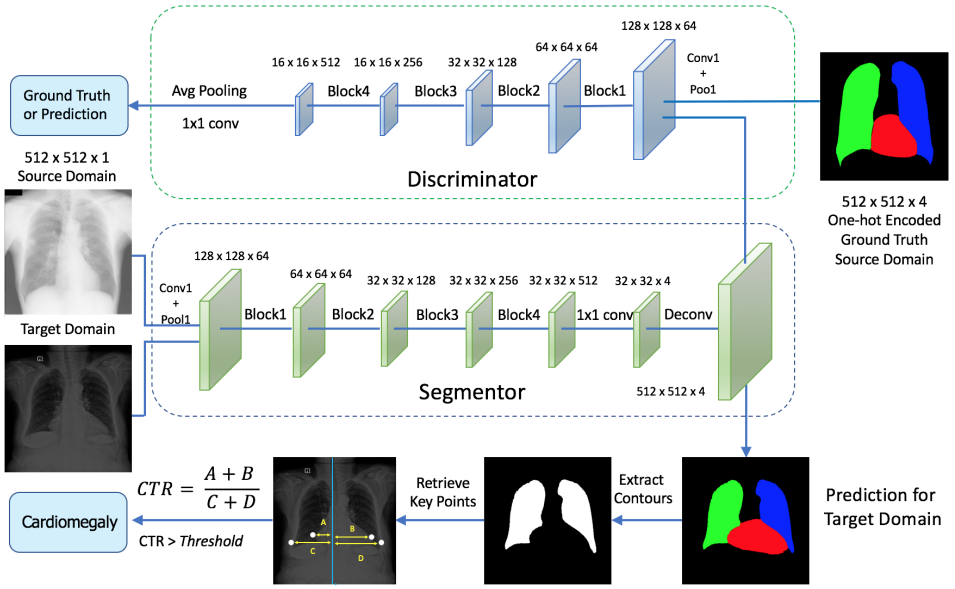

Figure 8.1: The segmentor produces the segmentation map, while the discriminator is trained to distinguish between predicted segmentation maps and ground truth prediction maps. The bottom part of the figure uses the prediction to perform cardiomegaly prediction.

estimate the cardiothoracic ratio, an indicator for cardiomegaly.

Contributions by the author

This work was performed while the author was in the Laboratory for Statistical Artificial InteLligence & INtegrative Genomics (SAILING Lab) at Carnegie Mellon University.

- The idea was developed in joint collaboration with Nanqing Dong and I devised the experiment setup.
- The paper manuscript was written in a joint effort with Nanqing Dong.

9

Paper IV

ConnNet: A Long-Range Relation-Aware Pixel-Connectivity Network for Salient Segmentation

Michael Kampffmeyer, Nanqing Dong, Xiaodan Liang, Yujia Zhang, and Eric P. Xing
Submitted to IEEE Transactions on Image Processing

Salient segmentation is a fundamental problem in image processing and provides the foundation of many tasks, such as object detection [Navalpakkam and Itti, 2006], video summarization [Ma et al., 2002] and face detection [Liu et al., 2017]. It is, therefore, crucial to achieve good performance on this task. Previous works in the past have mainly approached this task as a binary class segmentation task and relied on the use of FCNs. In this work, we instead investigate the use of connectivity modeling in order to improve salient segmentation performance and illustrate that our approach outperforms traditional segmentation based approaches. Figure 9.1 displays the motivation behind our approach. We predict if a given pixel is connected to its neighbors based on local and global relations between pixels

Connectivity prediction, by predicting for a given pixel the immediate neighbors, splits the segmentation task into subtasks. Each connectivity sub-task only aims to group pixels along a certain direction. Further, it is possible to view the technique from an ensemble viewpoint, as connectivity is a symmetric relation and neighboring pixels need to agree on whether or not they are connected to each other. This tends to provide more robust predictions.

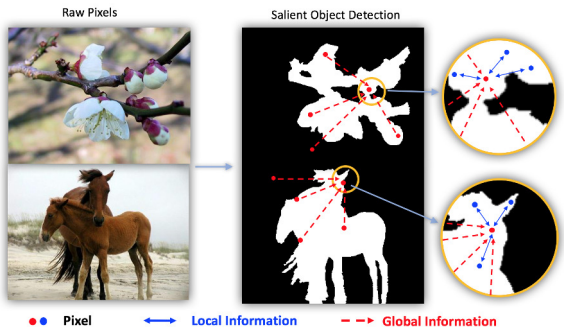

Figure 9.1: Salient objects can be found by modeling them as connected regions.

We extend the work to further evaluate connectivity modeling for the task of instance level salient segmentation by replacing the segmentation branch of a common instance (semantic) segmentation network with our proposed connectivity framework, achieving promising results.

Contributions by the author

This work was performed while the author was in the SAILING Lab at Carnegie Mellon University.

- The idea was developed in collaboration with Xiaodan Liang and Nanqing Dong.
- The implementation and experiments were conducted by Nanqing Dong and me.
- I wrote the manuscript draft of the paper.

10

Paper V

The Deep Kernelized Autoencoder

Michael Kampffmeyer, Sigurd Løkse, Filippo M Bianchi, Robert Jenssen, and Lorenzo Livi

Applied Soft Computing, 2018

In this work, we propose a new approach to representation learning (see Section 4.2). The method is based on the intuition that a meaningful learned representation in an Autoencoder (AE) should aim to preserve similarities from the input space. We introduce a novel regularization term that aligns the inner product between the codes with a kernel (similarity) matrix computed over the input space. Figure 10.1 illustrates the architecture.

While incorporating aspects of kernel methods, our approach is scalable as we propose mini-batch training. Through the regularization term, the AE is encouraged to learn an approximate explicit mapping from the input space to the code space, while the decoder learns an approximate explicit mapping from the code space back to input space. We illustrate in our experiments that our approach is able to learn useful representations both in a qualitative and quantitative manner.

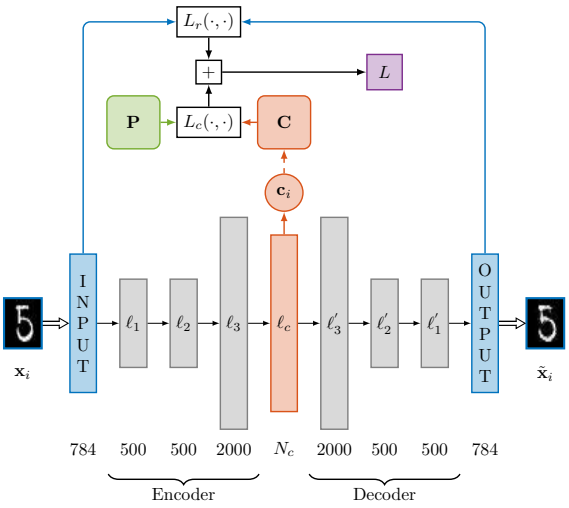

Figure 10.1: Architecture of the deep kernelized autoencoder. The inner products of the codes are aligned with a prior kernel that represents similarity in the input space. The overall loss is the combination of the reconstruction loss and the alignment cost.

Contributions by the author

- The idea was conceived in joint collaboration with all authors.
- The idea was developed by me with help of the co-authors.
- The implementation and experiments were conducted by me.
- I wrote the manuscript draft of the paper.

11

Paper VI

Deep Divergence-Based Approach to Clustering

Michael Kampffmeyer, Sigurd Løkse, Filippo M Bianchi, Lorenzo Livi, Arnt-Børre Salberg, and Robert Jenssen

Submitted to Neural Networks

This paper focuses on another unsupervised learning domain, namely clustering (see Section 4.3). In the presence of unlabeled data, we propose a neural network based method that finds the underlying structure in the data. We integrate ideas from both kernel methods and information theoretic learning by making use of the Cauchy-Schwartz divergence measure in order to encourage the underlying clusters to be compact and different clusters to be separate from each other. We illustrate this in Figure 11.1.

Using our proposed loss function, we are able to learn the representations of the neural network as well as discover an underlying clustering structure. Experimental results on a set of real and synthetic datasets show promising results and making use of mini-batch training, the proposed method scales well to large datasets.

Contributions by the author

- The idea was conceived in joint collaboration with all authors.

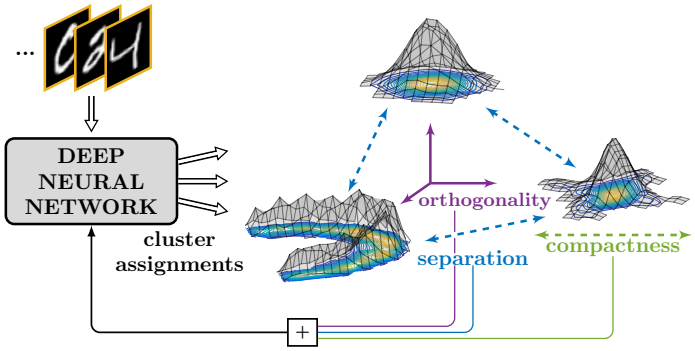

Figure 11.1: Concept figure of Paper VI. Our loss function is trained in order to produce compact clusters and at the same time force clusters to be separate from each other.

- The idea was developed by me with help of the co-authors.
- The implementation and experiments were conducted by me.
- I wrote the manuscript draft of the paper.

12

Paper VII

Rethinking Knowledge Graph Propagation for Zero-Shot Learning

Michael Kampffmeyer, Yinbo Chen, Xiaodan Liang, Hao Wang, Yujia Zhang, Eric P. Xing
Submitted to Neural Information Processing Systems 2018

In this work, we rethink the use of Graph Convolutional Neural Networks (GCNs) for zero-shot learning. GCNs have previously been used to address the zero-shot learning task as a semi-supervised learning task. The network is being trained to regress a set of classifier weights based on the classifiers from seen classes and the word embeddings from all the classes. A knowledge graph is used to represent relations between classes [Wang et al., 2018]. However, the propagation rule of the applied GCN can be viewed as performing a Laplacian smoothing operation at each graph layer Li et al. [2018a]. Smoothing, to some extent, is beneficial for semi-supervised classification, however, for the task of regression, this leads to information being diluted.

In order to address this problem, we propose a new way of utilizing GCNs for the task of zero-shot learning. We show that a single layer GCN outperforms deeper architectures as it limits information dilution. However, a single layer GCN only propagates information to immediate neighbors. To remedy this, we propose an Attentive Dense Graph Propagation Module, which exploits the knowledge graph by adding direct edges between a given node and its ancestors and descendants allowing information to propagate freely. We utilize a two-

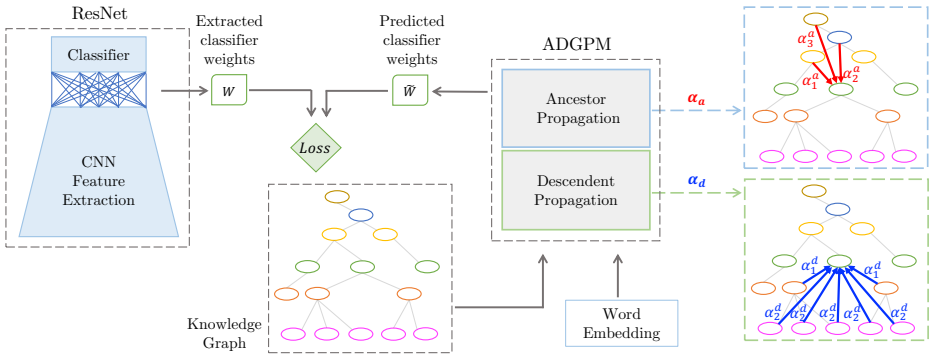

Figure 12.1: Architecture of our proposed approach for zero-shot learning. Given a knowledge graph and the word embedding of each class, our proposed Attentive Dense Graph Propagation Module (ADGPM) predicts the classifier weights for each class.

phase knowledge propagation procedure in order to share information between nodes efficiently and utilize a simple attention scheme to weigh the influence of neurons based on their graph distance from the node. Experimentally, we show the merits of the proposed approach, outperforming previously reported results. Figure 12.1 shows the overall architecture.

Contributions by the author

This work was performed while the author was in the SAILING Lab at Carnegie Mellon University.

- The idea was originally conceived by Xiaodan Liang and me and refined in collaboration with Yinbo Chen.
- I defined the experiment setup. Experiments were to a large extent performed by Yinbo Chen.
- I wrote the manuscript draft of the paper.

13

Conclusion

In this thesis, we advanced deep learning for semantic segmentation, mainly in the specific application domains of remote sensing and medical image analysis. The use of CNNs for urban land cover classification was investigated and the merits of using a weighted cross-entropy loss function to address class imbalance were explored. Since remote sensing often involves the fusion of multiple data sources, complications arise where certain modalities are missing. We illustrated approaches to handling missing modalities, especially targeted towards remote sensing. We quantified uncertainty in our segmentation prediction, in order to allow visualizations of the low-uncertainty predictions, and proposed an approach to unsupervised domain adaptation in order to perform segmentation for unlabeled images in the medical domain.

In the context of salient segmentation, we proposed a novel approach based on the idea that salient prediction can be modeled as a pixel-connectivity task and illustrated that we are able to outperform existing approaches while keeping the model relatively simple.

The other topic investigated in this thesis is the potential of deep learning for unsupervised settings. Besides the approach to unsupervised domain adaptation in the medical domain, we further proposed an approach to representation learning that incorporates ideas from kernel methods and is able to learn efficient representations by regularizing an autoencoder based on the similarity between data points. Furthermore, with help of ideas from kernel methods and information theoretic learning, we illustrated that deep neural networks can be

trained in an unsupervised manner to perform clustering, achieving promising results. Finally, we considered the task of zero-shot learning and illustrated that reconsidering the use of GCNs for the task, allows us to achieve state-of-the-art performance.

13.1 Future Directions

In this part, I would like to add my thoughts on the next steps for segmentation and unsupervised learning within deep learning.

Segmentation using deep learning approaches has been addressed by a large number of works in the past few years. However, there are still application-specific issues that need to be addressed. In the remote sensing domain, for instance, the use of deep learning techniques for hyperspectral images is underexplored. Most of these works, to my knowledge, are currently based on small (traditional) datasets and it would be useful to design models for large-scale hyperspectral image segmentation. One important direction related to this is the development of novel transfer learning and pretraining approaches for hyperspectral images. Further, labeling of datasets is a challenge and time-consuming. Accurate weakly-supervised and unsupervised approaches would be desirable to train networks for image segmentation.

Unsupervised deep learning is still in its infancy and I believe that, especially due to its potential, we will see large advances in this part of the field. Current method are often unstable or demand a delicate tuning of hyperparameters. Therefore an effort towards more stable methods should be made. This can be done by devising new cost-functions and regularization approaches as we have started doing in Paper VI, or by alternative approaches such as for instance meta-learning. I believe that incorporating more traditional machine learning concepts into deep learning architectures is a promising avenue, as they are well-understood and provide a more thorough theoretical foundation.

Part III

Included papers

14

Paper I

Semantic Segmentation of Small Objects and Modeling of Uncertainty in Urban Remote Sensing Images Using Deep Convolutional Neural Networks

Michael Kampffmeyer, Arnt-Børre Salberg, and Robert Jenssen

Proceedings of the IEEE Conference on Computer Vision and Pattern Recognition Workshops 2016

15

Paper II

Urban Land Cover Classification with Missing Data Modalities Using Deep Convolutional Neural Networks

Michael Kampffmeyer, Arnt-Børre Salberg, and Robert Jenssen

Journal of Selected Topics in Applied Earth Observations and Remote Sensing, 2018

16

Paper III

Unsupervised Domain Adaptation for Automatic Estimation of Cardiothoracic Ratio

Nanqing Dong, Michael Kampffmeyer, Xiaodan Liang, Zeya Wang, Wei Dai, Eric P. Xing

Proceedings of the International Conference on Medical Image Computing and Computer Assisted Intervention 2018

17

Paper IV

ConnNet: A Long-Range Relation-Aware Pixel-Connectivity Network for Salient Segmentation

Michael Kampffmeyer, Nanqing Dong, Xiaodan Liang, Yujia Zhang, and Eric P. Xing

Submitted to IEEE Transactions on Image Processing

18

Paper V

The Deep Kernelized Autoencoder

Michael Kampffmeyer, Sigurd Løkse, Filippo M Bianchi, Robert Jenssen, and Lorenzo Livi

Applied Soft Computing, 2018.

19

Paper VI

Deep Divergence-Based Approach to Clustering

Michael Kampffmeyer, Sigurd Løkse, Filippo M Bianchi, Lorenze Livi, Arnt-Børre Salberg, and Robert Jenssen

Submitted to Neural Networks

20

Paper VII

Rethinking Knowledge Graph Propagation for Zero-Shot Learning

Michael Kampffmeyer, Yinbo Chen, Xiaodan Liang, Hao Wang, Yujia Zhang, Eric P. Xing

Submitted to Neural Information Processing Systems 2018

Bibliography

Achanta, R., Hemami, S., Estrada, F., and Susstrunk, S. (2009). Frequency-tuned salient region detection. In *Computer vision and pattern recognition, 2009. cvpr 2009. ieee conference on*, pages 1597–1604. IEEE.

Akata, Z., Perronnin, F., Harchaoui, Z., and Schmid, C. (2013). Label-embedding for attribute-based classification. In *Computer Vision and Pattern Recognition (CVPR), 2013 IEEE Conference on*, pages 819–826. IEEE.

Akata, Z., Reed, S., Walter, D., Lee, H., and Schiele, B. (2015). Evaluation of output embeddings for fine-grained image classification. In *Proceedings of the IEEE Conference on Computer Vision and Pattern Recognition*, pages 2927–2936.

Arbeláez, P., Pont-Tuset, J., Barron, J. T., Marques, F., and Malik, J. (2014). Multiscale combinatorial grouping. In *Proceedings of the IEEE conference on computer vision and pattern recognition*, pages 328–335.

Arjovsky, M., Chintala, S., and Bottou, L. (2017). Wasserstein generative adversarial networks. In *International Conference on Machine Learning*, pages 214–223.

Badrinarayanan, V., Kendall, A., and Cipolla, R. (2015). Segnet: A deep convolutional encoder-decoder architecture for image segmentation. *arXiv preprint arXiv:1511.00561*.

Bahdanau, D., Chorowski, J., Serdyuk, D., Brakel, P., and Bengio, Y. (2016). End-to-end attention-based large vocabulary speech recognition. In *Acoustics, Speech and Signal Processing (ICASSP), 2016 IEEE International Conference on*, pages 4945–4949. IEEE.

Baldi, P. and Hornik, K. (1989). Neural networks and principal component analysis: Learning from examples without local minima. *Neural networks*, 2(1):53–58.

Ballard, D. H. (1987). Modular learning in neural networks. In *AAAI*, pages 279–284.

Bamberger, R. H. and Smith, M. J. (1992). A filter bank for the directional decomposition of images: Theory and design. *IEEE transactions on signal processing*, 40(4):882–893.

Bengio, Y., Courville, A., and Vincent, P. (2013). Representation learning: A review and new perspectives. *Pattern Analysis and Machine Intelligence, IEEE Transactions on*, 35(8):1798–1828.

Bianchi, F. M., Maiorino, E., Kampffmeyer, M. C., Rizzi, A., and Jenssen, R. (2017). *Recurrent Neural Networks for Short-Term Load Forecasting: An Overview and Comparative Analysis*. Springer.

Boser, B. E., Guyon, I. M., and Vapnik, V. N. (1992). A training algorithm for optimal margin classifiers. In *Proceedings of the fifth annual workshop on Computational learning theory*, pages 144–152. ACM.

Bruna, J., Zaremba, W., Szlam, A., and LeCun, Y. (2014). Spectral networks and locally connected networks on graphs. *International Conference on Learning Representations*.

Carreira, J., Caseiro, R., Batista, J., and Sminchisescu, C. (2012). Semantic segmentation with second-order pooling. In *European Conference on Computer Vision*, pages 430–443. Springer.

Carreira, J. and Sminchisescu, C. (2011). Cpmc: Automatic object segmentation using constrained parametric min-cuts. *IEEE Transactions on Pattern Analysis & Machine Intelligence*, (7):1312–1328.

Chang, S., Zhang, Y., Han, W., Yu, M., Guo, X., Tan, W., Cui, X., Witbrock, M., Hasegawa-Johnson, M. A., and Huang, T. S. (2017). Dilated recurrent neural networks. In *Advances in Neural Information Processing Systems*, pages 77–87.

Chen, L.-C., Papandreou, G., Kokkinos, I., Murphy, K., and Yuille, A. L. (2018). Deeplab: Semantic image segmentation with deep convolutional nets, atrous convolution, and fully connected crfs. *IEEE transactions on pattern analysis and machine intelligence*, 40(4):834–848.

Chen, L.-C., Papandreou, G., Schroff, F., and Adam, H. (2017). Rethinking atrous convolution for semantic image segmentation. *arXiv preprint arXiv:1706.05587*.

Chen, Y. and Lee, J. (2012). Ulcer detection in wireless capsule endoscopy video. In *Proceedings of the 20th ACM international conference on Multimedia*, pages 1181–1184. ACM.

Cheng, M.-M., Mitra, N. J., Huang, X., Torr, P. H., and Hu, S.-M. (2015). Global contrast based salient region detection. *Transactions on Pattern Analysis and Machine Intelligence*, 37(3):569–582.

Choromanska, A., Henaff, M., Mathieu, M., Arous, G. B., and LeCun, Y. (2014). The loss surface of multilayer networks. *arXiv preprint arXiv:1412.0233*.

Ciresan, D., Giusti, A., Gambardella, L. M., and Schmidhuber, J. (2012). Deep neural networks segment neuronal membranes in electron microscopy images. In *Advances in neural information processing systems*, pages 2843–2851.

Comaniciu, D. and Meer, P. (2002). Mean shift: A robust approach toward feature space analysis. *IEEE Transactions on pattern analysis and machine intelligence*, 24(5):603–619.

Cover, T. M. and Thomas, J. A. (1991). *Elements of Information Theory*. Wiley, New York.

Cramer, M. (2010). The dgpf-test on digital airborne camera evaluation–overview and test design. *Photogrammetrie-Fernerkundung-Geoinformation*, 2010(2):73–82.

Dahl, G. E., Ranzato, M., Mohamed, A.-r., and Hinton, G. (2010). Phone recognition with the mean-covariance restricted boltzmann machine. In *Proceedings of the 23rd International Conference on Neural Information Processing Systems-Volume 1*, pages 469–477.

Dahl, G. E., Yu, D., Deng, L., and Acero, A. (2012). Context-dependent pre-trained deep neural networks for large-vocabulary speech recognition. *IEEE Transactions on audio, speech, and language processing*, 20(1):30–42.

Dai, J., He, K., Li, Y., Ren, S., and Sun, J. (2016a). Instance-sensitive fully convolutional networks. In *Proceedings of the European Conference on Computer Vision*, pages 534–549. Springer.

Dai, J., He, K., and Sun, J. (2016b). Instance-aware semantic segmentation via multi-task network cascades. In *Proceedings of the IEEE Conference on Computer Vision and Pattern Recognition*, pages 3150–3158.

Dauphin, Y. N., Pascanu, R., Gulcehre, C., Cho, K., Ganguli, S., and Bengio,

Y. (2014). Identifying and attacking the saddle point problem in high-dimensional non-convex optimization. In *Advances in Neural Information Processing Systems*, pages 2933–2941.

Defferrard, M., Bresson, X., and Vandergheynst, P. (2016). Convolutional neural networks on graphs with fast localized spectral filtering. In *Advances in Neural Information Processing Systems*, pages 3844–3852.

Dempster, A. P., Laird, N. M., and Rubin, D. B. (1977). Maximum likelihood from incomplete data via the em algorithm. *Journal of the royal statistical society. Series B (methodological)*, pages 1–38.

Dong, N., Kampffmeyer, M., Liang, X., Wang, Z., Dai, W., and Xing, E. P. (2018). Reinforced auto-zoom net: Towards accurate and fast breast cancer segmentation in whole-slide images. *arXiv preprint arXiv:1807.11113*.

Duchi, J., Hazan, E., and Singer, Y. (2011). Adaptive subgradient methods for online learning and stochastic optimization. *Journal of Machine Learning Research*, 12(Jul):2121–2159.

Duvenaud, D. K., Maclaurin, D., Iparraguirre, J., Bombarell, R., Hirzel, T., Aspuru-Guzik, A., and Adams, R. P. (2015). Convolutional networks on graphs for learning molecular fingerprints. In *Advances in neural information processing systems*, pages 2224–2232.

Eisen, M. B., Spellman, P. T., Brown, P. O., and Botstein, D. (1998). Cluster analysis and display of genome-wide expression patterns. *Proceedings of the National Academy of Sciences*, 95(25):14863–14868.

Esteva, A., Kuprel, B., Novoa, R. A., Ko, J., Swetter, S. M., Blau, H. M., and Thrun, S. (2017). Dermatologist-level classification of skin cancer with deep neural networks. *Nature*, 542(7639):115.

Everingham, M., Eslami, S. M. A., Van Gool, L., Williams, C. K. I., Winn, J., and Zisserman, A. (2015). The pascal visual object classes challenge: A retrospective. *International Journal of Computer Vision*, 111(1):98–136.

Farabet, C., Couprie, C., Najman, L., and LeCun, Y. (2013). Learning hierarchical features for scene labeling. *Pattern Analysis and Machine Intelligence, IEEE Transactions on*, 35(8):1915–1929.

Frome, A., Corrado, G. S., Shlens, J., Bengio, S., Dean, J., Mikolov, T., et al. (2013). Devise: A deep visual-semantic embedding model. In *Advances in Neural Information Processing Systems*, pages 2121–2129.

Fulkerson, B., Vedaldi, A., and Soatto, S. (2009). Class segmentation and object localization with superpixel neighborhoods. In *Computer Vision, 2009 IEEE 12th International Conference on*, pages 670–677. IEEE.

Girshick, R. (2015). Fast r-cnn. In *Proceedings of the IEEE International Conference on Computer Vision*, pages 1440–1448.

Glorot, X., Bordes, A., and Bengio, Y. (2011). Deep sparse rectifier neural networks. In *International Conference on Artificial Intelligence and Statistics*, pages 315–323.

Goodfellow, I. (2016). Nips 2016 tutorial: Generative adversarial networks. *arXiv preprint arXiv:1701.00160*.

Goodfellow, I., Pouget-Abadie, J., Mirza, M., Xu, B., Warde-Farley, D., Ozair, S., Courville, A., and Bengio, Y. (2014). Generative adversarial nets. In *NIPS*, pages 2672–2680.

Gretton, A., Smola, A., Huang, J., Schmittfull, M., Borgwardt, K., and Schölkopf, B. (2009). *Covariate shift and local learning by distribution matching*, pages 131–160. MIT Press, Cambridge, MA, USA.

Hammond, D. K., Vandergheynst, P., and Gribonval, R. (2011). Wavelets on graphs via spectral graph theory. *Applied and Computational Harmonic Analysis*, 30(2):129–150.

He, K., Gkioxari, G., Dollár, P., and Girshick, R. (2017). Mask r-cnn. In *Proceedings of the IEEE international conference on computer vision*, pages 2980–2988. IEEE.

He, K., Zhang, X., Ren, S., and Sun, J. (2016). Deep residual learning for image recognition. In *Proceedings of the IEEE Conference on Computer Vision and Pattern Recognition*, pages 770–778. IEEE.

Hinton, G. (2002). Training products of experts by minimizing contrastive divergence. *Neural computation*, 14(8):1771–1800.

Hinton, G. (2010). A practical guide to training restricted Boltzmann machines. *Momentum*, 9(1):926.

Hinton, G., Deng, L., Yu, D., Dahl, G. E., Mohamed, A.-r., Jaitly, N., Senior, A., Vanhoucke, V., Nguyen, P., Sainath, T. N., et al. (2012). Deep neural networks for acoustic modeling in speech recognition: The shared views of four research groups. *IEEE Signal processing magazine*, 29(6):82–97.

Hinton, G. E., Osindero, S., and Teh, Y.-W. (2006). A fast learning algorithm for deep belief nets. *Neural computation*, 18(7):1527–1554.

Ho, T. K. (1995). Random decision forests. In *Document analysis and recognition, 1995., proceedings of the third international conference on*, volume 1, pages 278–282. IEEE.

Hodge, V. and Austin, J. (2004). A survey of outlier detection methodologies. *Artificial intelligence review*, 22(2):85–126.

Hoffman, J., Gupta, S., and Darrell, T. (2016). Learning with side information through modality hallucination. In *Proceedings of the IEEE Conference on Computer Vision and Pattern Recognition*, pages 826–834.

Jain, A. K. (2010). Data clustering: 50 years beyond k-means. *Pattern recognition letters*, 31(8):651–666.

Japkowicz, N., Hanson, S. J., and Gluck, M. A. (2000). Nonlinear autoassociation is not equivalent to pca. *Neural computation*, 12(3):531–545.

Jenssen, R., Principe, J. C., Erdogmus, D., and Eltoft, T. (2006). The cauchy–schwarz divergence and parzen windowing: Connections to graph theory and mercer kernels. *Journal of the Franklin Institute*, 343(6):614–629.

Johnson-Roberson, M., Barto, C., Mehta, R., Sridhar, S. N., Rosaen, K., and Vasudevan, R. (2017). Driving in the matrix: Can virtual worlds replace human-generated annotations for real world tasks? In *Robotics and Automation (ICRA), 2017 IEEE International Conference on*, pages 746–753. IEEE.

Karpathy, A., Toderici, G., Shetty, S., Leung, T., Sukthankar, R., and Fei-Fei, L. (2014). Large-scale video classification with convolutional neural networks. In *Proceedings of the IEEE conference on Computer Vision and Pattern Recognition*, pages 1725–1732.

Kingma, D. and Ba, J. (2015). Adam: A method for stochastic optimization. In *International Conference on Learning Representations*.

Kingma, D. P. and Welling, M. (2014). Auto-encoding variational bayes. *International Conference on Learning Representations*.

Kipf, T. N. and Welling, M. (2017). Semi-supervised classification with graph convolutional networks. In *International Conference for Learning Representation*.

Krizhevsky, A., Sutskever, I., and Hinton, G. E. (2012). Imagenet classification with deep convolutional neural networks. In *Advances in neural information processing systems*, pages 1097–1105.

LeCun, Y., Bengio, Y., and Hinton, G. (2015). Deep learning. *Nature*, 521(7553):436–444.

Leung, T. and Malik, J. (2001). Representing and recognizing the visual appearance of materials using three-dimensional textons. *International journal of computer vision*, 43(1):29–44.

Li, G., Xie, Y., Lin, L., and Yu, Y. (2017). Instance-level salient object segmentations. In *Proceedings of the IEEE Conference on Computer Vision and Pattern Recognition*. IEEE.

Li, G. and Yu, Y. (2015). Visual saliency based on multiscale deep features. In *Proceedings of the IEEE Conference on Computer Vision and Pattern Recognition*, pages 5455–5463. IEEE.

Li, G. and Yu, Y. (2016). Deep contrast learning for salient object detection. In *Proceedings of the IEEE Conference on Computer Vision and Pattern Recognition*, pages 478–487. IEEE.

Li, Q., Han, Z., and Wu, X.-M. (2018a). Deeper insights into graph convolutional networks for semi-supervised learning. In *Proceedings of the 33rd national conference on Artificial intelligence*. AAAI Press.

Li, Y., Zhang, J., Zhang, J., and Huang, K. (2018b). Discriminative learning of latent features for zero-shot recognition. In *Proceedings of the IEEE Conference on Computer Vision and Pattern Recognition*, pages 7463–7471.

Litjens, G., Kooi, T., Bejnordi, B. E., Setio, A. A. A., Ciompi, F., Ghafoorian, M., van der Laak, J. A., Van Ginneken, B., and Sánchez, C. I. (2017). A survey on deep learning in medical image analysis. *Medical image analysis*, 42:60–88.

Liu, T., Yuan, Z., Sun, J., Wang, J., Zheng, N., Tang, X., and Shum, H.-Y. (2011). Learning to detect a salient object. *Transactions on Pattern Analysis and Machine Intelligence*, 33(2):353–367.

Liu, Y., Zhang, S., Xu, M., and He, X. (2017). Predicting salient face in multiple-face videos. In *Proceedings of the IEEE Conference on Computer Vision and Pattern Recognition*, pages 4420–4428. IEEE.

Long, J., Shelhamer, E., and Darrell, T. (2015a). Fully convolutional networks

for semantic segmentation. In *Proceedings of the IEEE Conference on Computer Vision and Pattern Recognition*, pages 3431–3440.

Long, M., Cao, Y., Wang, J., and Jordan, M. I. (2015b). Learning transferable features with deep adaptation networks. In *Proceedings of the 32nd International Conference on International Conference on Machine Learning-Volume 37*, pages 97–105. JMLR. org.

Ma, Y.-F., Lu, L., Zhang, H.-J., and Li, M. (2002). A user attention model for video summarization. In *Proceedings of the tenth ACM international conference on Multimedia*, pages 533–542. ACM.

MacQueen, J. (1967). Some methods for classification and analysis of multivariate observations. In *Proceedings of the fifth Berkeley symposium on mathematical statistics and probability*, volume 1, pages 281–297. Oakland, CA, USA.

Maggiori, E., Tarabalka, Y., Charpiat, G., and Alliez, P. (2017). Convolutional neural networks for large-scale remote-sensing image classification. *IEEE Transactions on Geoscience and Remote Sensing*, 55(2):645–657.

Marmanis, D., Schindler, K., Wegner, J. D., Galliani, S., Datcu, M., and Stilla, U. (2018). Classification with an edge: Improving semantic image segmentation with boundary detection. *ISPRS Journal of Photogrammetry and Remote Sensing*, 135:158–172.

Mercer, J. (1909). Functions of positive and negative type, and their connection with the theory of integral equations. *Proceedings of the Royal Society of London Series A*, 83:69–70.

Mikolov, T., Chen, K., Corrado, G., and Dean, J. (2013). Efficient estimation of word representations in vector space. *arXiv preprint arXiv:1301.3781*.

Minsky, M. and Seymour, P. (1969). *Perceptrons*. MIT press.

Mohamed, A.-r., Dahl, G. E., and Hinton, G. (2012). Acoustic modeling using deep belief networks. *IEEE Trans. Audio, Speech & Language Processing*, 20(1):14–22.

Montavon, G., Orr, G., and Müller, K.-R. (2012). *Neural Networks: Tricks of the Trade*, volume 7700. Springer.

Mostajabi, M., Yadollahpour, P., and Shakhnarovich, G. (2015). Feedforward semantic segmentation with zoom-out features. In *Proceedings of the IEEE*

conference on computer vision and pattern recognition, pages 3376–3385.

Navalpakkam, V. and Itti, L. (2006). An integrated model of top-down and bottom-up attention for optimizing detection speed. In *Proceedings of the IEEE Conference on Computer Vision and Pattern Recognition*, volume 2, pages 2049–2056. IEEE.

Norouzi, M., Mikolov, T., Bengio, S., Singer, Y., Shlens, J., Frome, A., Corrado, G. S., and Dean, J. (2014). Zero-shot learning by convex combination of semantic embeddings. *International Conference for Learning Representation*.

Olshausen, B. A. and Field, D. J. (1996). Emergence of simple-cell receptive field properties by learning a sparse code for natural images. *Nature*, 381(6583):607.

Parikh, D. and Grauman, K. (2011). Relative attributes. In *Computer Vision (ICCV), 2011 IEEE International Conference on*, pages 503–510. IEEE.

Perazzi, F., Krähenbühl, P., Pritch, Y., and Hornung, A. (2012). Saliency filters: Contrast based filtering for salient region detection. In *Proceedings of the IEEE Conference on Computer Vision and Pattern Recognition*, pages 733–740. IEEE.

Pinheiro, P. O., Collobert, R., and Dollár, P. (2015). Learning to segment object candidates. In *Advances in Neural Information Processing Systems*, pages 1990–1998.

Principe, J. C. (2010). *Information theoretic learning: Renyi's entropy and kernel perspectives*. Springer Science & Business Media.

Principe, J. C. and Xu, D. (2000). Information theoretic learning. *Unsupervised adaptive filtering*.

Radford, A., Metz, L., and Chintala, S. (2016). Unsupervised representation learning with deep convolutional generative adversarial networks. *International Conference for Learning Representation Workshop*.

Ranzato, M., Poultney, C., Chopra, S., and Cun, Y. L. (2007). Efficient learning of sparse representations with an energy-based model. In *Advances in neural information processing systems*, pages 1137–1144.

Ren, S., He, K., Girshick, R., and Sun, J. (2015). Faster r-cnn: Towards real-time object detection with region proposal networks. In *Advances in Neural Information Processing Systems*, pages 91–99.

Ren, S., He, K., Girshick, R., and Sun, J. (2017). Faster r-cnn: towards real-time object detection with region proposal networks. *Transactions on Pattern Analysis and Machine Intelligence*, 39(6):1137–1149.

Rifai, S., Mesnil, G., Vincent, P., Muller, X., Bengio, Y., Dauphin, Y., and Glorot, X. (2011a). Higher order contractive auto-encoder. In *Machine Learning and Knowledge Discovery in Databases*, pages 645–660. Springer.

Rifai, S., Vincent, P., Muller, X., Glorot, X., and Bengio, Y. (2011b). Contractive auto-encoders: Explicit invariance during feature extraction. In *Proceedings of the 28th International Conference on International Conference on Machine Learning*, pages 833–840. Omnipress.

Romera-Paredes, B. and Torr, P. (2015). An embarrassingly simple approach to zero-shot learning. In *International Conference on Machine Learning*, pages 2152–2161.

Rosenblatt, F. (1958). The perceptron: a probabilistic model for information storage and organization in the brain. *Psychological review*, 65(6):386.

Ruder, S. (2016). An overview of gradient descent optimization algorithms. *arXiv preprint arXiv:1609.04747*.

Rumelhart, D. E., Hinton, G. E., and Williams, R. J. (1986). Learning representations by back-propagating errors. *nature*, 323(6088):533.

Sahami, M. and Koller, D. (1998). *Using machine learning to improve information access*. PhD thesis, Stanford University, Department of Computer Science.

Salakhutdinov, R., Mnih, A., and Hinton, G. (2007). Restricted Boltzmann machines for collaborative filtering. In *Proceedings of the 24th international conference on Machine learning*, pages 791–798. ACM.

Salberg, A.-B., Trier, Ø. D., and Kampffmeyer, M. (2017). Large-scale mapping of small roads in lidar images using deep convolutional neural networks. In *Scandinavian Conference on Image Analysis*, pages 193–204. Springer.

Sermanet, P., Eigen, D., Zhang, X., Mathieu, M., Fergus, R., and LeCun, Y. (2014). Overfeat: Integrated recognition, localization and detection using convolutional networks. *International Conference on Learning Representations*.

Sharma, A. and Ghosh, J. (2015). Saliency based segmentation of satellite images. *ISPRS Annals of Photogrammetry, Remote Sensing & Spatial Information Sciences*, 2.

Shawe-Taylor, J. and Cristianini, N. (2004). *Kernel methods for pattern analysis*. Cambridge university press.

Shotton, J., Fitzgibbon, A., Cook, M., Sharp, T., Finocchio, M., Moore, R., Kipman, A., and Blake, A. (2011). Real-time human pose recognition in parts from single depth images. In *Computer Vision and Pattern Recognition (CVPR), 2011 IEEE Conference on*, pages 1297–1304. Ieee.

Shotton, J., Johnson, M., and Cipolla, R. (2008). Semantic texton forests for image categorization and segmentation. In *Computer vision and pattern recognition, 2008. CVPR 2008. IEEE Conference on*, pages 1–8. IEEE.

Smolensky, P. (1986). Information processing in dynamical systems: Foundations of harmony theory. Technical report, COLORADO UNIV AT BOULDER DEPT OF COMPUTER SCIENCE.

Socher, R., Ganjoo, M., Manning, C. D., and Ng, A. (2013). Zero-shot learning through cross-modal transfer. In *Advances in Neural Information Processing Systems*, pages 935–943.

Sokal, R. R. (1963). The principles and practice of numerical taxonomy. *Taxon*, pages 190–199.

Srivastava, N., Hinton, G., Krizhevsky, A., Sutskever, I., and Salakhutdinov, R. (2014). Dropout: A simple way to prevent neural networks from overfitting. *The Journal of Machine Learning Research*, 15(1):1929–1958.

Tian, F., Gao, B., Cui, Q., Chen, E., and Liu, T.-Y. (2014). Learning deep representations for graph clustering. In *AAAI*, pages 1293–1299.

Tzeng, E., Hoffman, J., Saenko, K., and Darrell, T. (2017). Adversarial discriminative domain adaptation. In *CVPR*, pages 2962–2971. IEEE.

Tzeng, E., Hoffman, J., Zhang, N., Saenko, K., and Darrell, T. (2014). Deep domain confusion: Maximizing for domain invariance. *arXiv preprint arXiv:1412.3474*.

Ungar, L. H. and Foster, D. P. (1998). Clustering methods for collaborative filtering. In *AAAI workshop on recommendation systems*, volume 1, pages 114–129.

Valenti, R., Sebe, N., and Gevers, T. (2009). Image saliency by isocentric curvedness and color. In *Proceedings of the IEEE international conference on computer vision*, pages 2185–2192. IEEE.

Vincent, P., Larochelle, H., Lajoie, I., Bengio, Y., and Manzagol, P.-A. (2010). Stacked denoising autoencoders: Learning useful representations in a deep network with a local denoising criterion. *Journal of machine learning research*, 11(Dec):3371–3408.

Wang, L., Lu, H., Ruan, X., and Yang, M.-H. (2015). Deep networks for saliency detection via local estimation and global search. In *Proceedings of the IEEE Conference on Computer Vision and Pattern Recognition*, pages 3183–3192. IEEE.

Wang, X., Ye, Y., and Gupta, A. (2018). Zero-shot recognition via semantic embeddings and knowledge graphs. In *arXiv preprint arXiv:1803.08035*.

Xie, J., Girshick, R., and Farhadi, A. (2016). Unsupervised deep embedding for clustering analysis. In *International conference on machine learning*, pages 478–487.

Zhang, J., Sclaroff, S., Lin, Z., Shen, X., Price, B., and Mech, R. (2016). Unconstrained salient object detection via proposal subset optimization. In *Proceedings of the IEEE conference on computer vision and pattern recognition*, pages 5733–5742.

Zhang, L., Xiang, T., and Gong, S. (2017). Learning a deep embedding model for zero-shot learning. In *Computer Vision and Pattern Recognition (CVPR), 2017 IEEE Conference on*, pages 3010–3019. IEEE.

Zhang, Y., Kampffmeyer, M., Liang, X., Tan, M., and Xing, E. P. (2018a). Query-conditioned three-player adversarial network for video summarization. *arXiv preprint arXiv:1807.06677*.

Zhang, Y., Kampffmeyer, M., Liang, X., Zhang, D., Tan, M., and Xing, E. P. (2018b). Dtr-gan: Dilated temporal relational adversarial network for video summarization. *arXiv preprint arXiv:1804.11228*.

Zhu, X. X., Tuia, D., Mou, L., Xia, G.-S., Zhang, L., Xu, F., and Fraundorfer, F. (2017). Deep learning in remote sensing: a comprehensive review and list of resources. *IEEE Geoscience and Remote Sensing Magazine*, 5(4):8–36.